Tectonic and chronostratigraphic implications of new ^{40}Ar/^{39}Ar geochronology and geochemistry of the Arman and Maltan-Ola volcanic fields, Okhotsk-Chukotka volcanic belt, northeastern Russia

Jeremy K. Hourigan[†]
Department of Geological and Environmental Sciences, Stanford University, Stanford, California 94305, USA

Vyacheslav V. Akinin[‡]
North East Interdisciplinary Scientific Research Institute, Far East Branch, Russian Academy of Sciences, Magadan, Portovaya Ulitsa, 16, 685000, Russia

ABSTRACT

The Okhotsk-Chukotka volcanic belt is part of an extensive late Early to Late Cretaceous Andean-style magmatic arc that spans the entire eastern margin of the Asian continent. The belt itself stretches 3000 km from the Chukotka Peninsula to the Uda River and comprises ~1.2 × 10^6 km^3 of volcanic rock over a 500,000 km^2 area. Despite its size and regional tectonic significance, the time span of magmatic activity is poorly constrained and the subject of significant debate, mostly in the Russian literature. In this paper, we provide new geochronologic control on the timing of inception and cessation of magmatism for the Arman and Maltan-Ola volcanic fields. These field localities were chosen because they are well studied, relatively accessible, and contain floral assemblages that have been used to correlate volcanic sequences at the regional scale. The majority of the volcanic sequence was emplaced between 85.5 ± 1.3 Ma and 74.0 ± 1.2 Ma, as shown by 17 new ^{40}Ar/^{39}Ar ages. The Coniacian–Santonian to Campanian age range indicated is 15 m.y. younger than the Albian to early Cenomanian age range given by a synthesis of floral stratigraphic, K-Ar, and Rb-Sr geochronologic data. The calc-alkaline part of the volcanic section spans an apparent age range of 85.5 ± 1.3 Ma to 80.7 ± 0.8 Ma. Capping basalts were emplaced between 77.5 ± 1.1 Ma and 74.0 ± 1.2 Ma and exhibit a within-plate geochemical signature, which we attribute to a temporally and geochemically distinct, possibly extension-related, phase of magmatism. The apparent northwestward migration of the arc front from the interior (seaward) zone (Taigonos Peninsula, Magadan batholith) in Albian–Cenomanian time to the Arman and Maltan-Ola volcanic fields in Coniacian–Santonian to Campanian time may be explained by shallowing of the subducting paleo-Pacific (Kula?) oceanic plate.

The flat-lying nature of these volcanic rocks and the within-plate geochemical affinity of the capping basalt unit are inconsistent with prevailing tectonic models for the cessation of arc magmatism and formation of the Sea of Okhotsk which require the collision of a microcontinental block or oceanic plateau with the northeast Asian margin in the Late Cretaceous.

Keywords: Okhotsk-Chukotka volcanic belt, northeast Russia, geochronology, Cretaceous, subduction-related magmatism.

INTRODUCTION

The chronostratigraphy of the Okhotsk-Chukotka volcanic belt (Fig. 1) is one of the most debated topics in the geology of the Russian Far East. To date, research constraining the age of the volcanic section of the Okhotsk-Chukotka volcanic belt has focused on phytostratigraphic or K-Ar and Rb-Sr whole-rock dating methods (e.g., Belyi, 1994; Kotlyar et al., 2001) (Fig. 2).[1] It is generally accepted in the literature that the volcanism occurred in middle Albian to early Campanian time (Belyi, 1994). However, an often-significant disparity between the phytostratigraphic age of sedimentary rocks and the isotopic age of intercalated volcanic flow units continues to fuel this debate (Belyy, 1982).

A better understanding of the tectonic and magmatic evolution of northeast Russia requires improved resolution of the chronostratigraphy of the Okhotsk-Chukotka volcanic belt, and ^{40}Ar/^{39}Ar geochronology is ideally suited to accomplish this task. Unlike Rb-Sr and K-Ar, ^{40}Ar/^{39}Ar stepwise-heating experiments afford detailed information about the distribution and retentivity of radiogenic isotopes in monomineralic separates. The concordance of inverse-isochron ages and spectrum ages provides an additional internal check on data quality and closed-system behavior.

The timing and time vs. space patterns of magmatism within the Okhotsk-Chukotka volcanic belt are critical to our understanding of the evolution of the northeast Asian convergent margin. With limited preservation and

---

[†]Present address: Department of Geology and Geophysics, Yale University, P.O. Box 208109, New Haven, Connecticut 06520-8109, USA; e-mail: jeremy.hourigan@yale.edu.
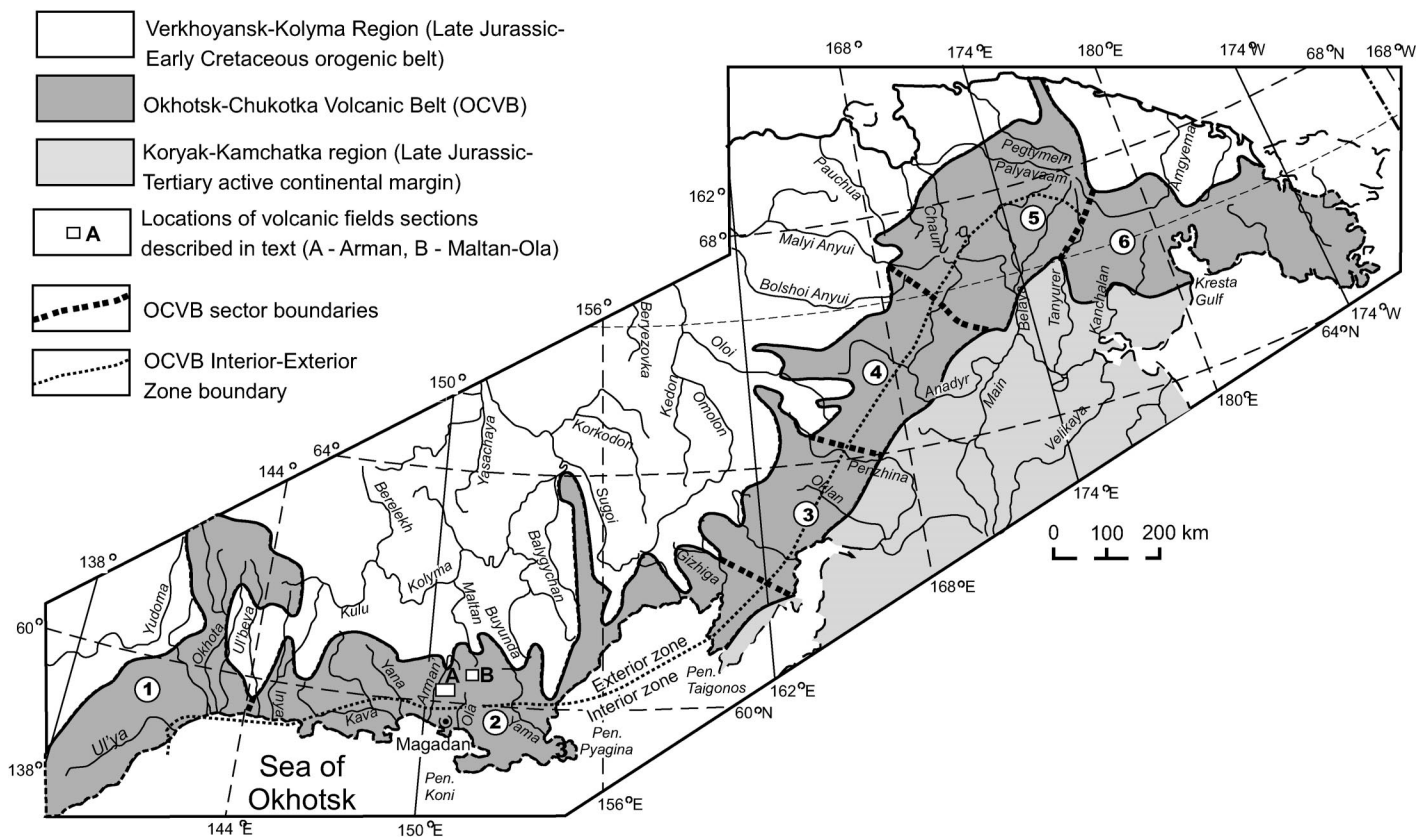
[‡]E-mail: akinin@neisri.ru.

Figure 1. Index map for the Okhotsk-Chukotka volcanic belt (OCVB), showing the distribution of late Early to Late Cretaceous volcanic and plutonic rocks and location of volcano-stratigraphic sections described in the text. Numbered circles indicate the locations of "sectors" of the Okhotsk-Chukotka volcanic belt: 1—Western Okhotsk; 2—Okhotsk; 3—Penzhina; 4—Anadyr; 5—Central Chukotka; 6—Eastern Chukotka.

inaccessible exposures of the forearc and accretionary-wedge parts of the margin, knowledge about the interaction of the plates of the paleo-Pacific and the northeast Russian margin must be drawn from the magmatic record. A key problem in the central part of the volcanic belt is the mechanism responsible for cessation of arc magmatism. The predominant theory holds that arc cessation occurred following collision of a microcontinental block or oceanic plateau that was incapable of continued subduction (Parfenov and Natal'in, 1977; Watson and Fujita, 1985; Zonenshain et al., 1990; Şengör and Natal'in, 1996; Bogdanov and Dobretsov, 2002). This model arose as an explanation for the shallowly submerged, moderately thick (~30 km), block-like basement of the Sea of Okhotsk (e.g., Gnibidenko and Khvedchuk, 1982) and the migration of the magmatic front and locus of accretion-related deformation to Kamchatka in the early Tertiary (Parfenov and Natal'in, 1977; Watson and Fujita, 1985). The age range, degree of deformation, and petrogenetic nature of eruptive products and the timing of

cessation of the Okhotsk-Chukotka volcanic belt in the Okhotsk sector are key pieces of information needed to test the validity of the block-collision models for the origin of the Sea of Okhotsk and the termination of arc magmatism.

We report 17 new $^{40}Ar/^{39}Ar$ ages from the Maltan-Ola and Arman volcanic fields in the Okhotsk segment of the Okhotsk-Chukotka volcanic belt. This study is the first of its kind to address systematically the age of volcanic units over the entire stratigraphic sequence of a volcanic field within the volcanic belt. Samples were collected during the course of two summer field expeditions in 1996 and 1998 as part of a collaborative effort between Stanford University and the North East Interdisciplinary Scientific Research Institute. Our samples come from two stratigraphic sections within the Arman volcanic field (Fig. 1) and a single section in the Kheta River region in the Maltan-Ola volcanic field (Fig. 1). The Arman and Maltan-Ola volcanic fields, because of their proximity to Magadan and their accessibility via roads and traversable river valleys,

are perhaps the best studied volcanic fields of the Okhotsk-Chukotka volcanic belt. The volcano-stratigraphic successions of these fields are thought to be typical of the volcanic stratigraphy of other fields within the Okhotsk sector of the belt (Belyi, 1977) (Fig. 1). In addition, associated sedimentary rocks in these fields are known to contain Arman and Arkagala floral complexes (Fig. 2), which are recognized throughout the Okhotsk-Chukotka volcanic belt and together form a widely used standard for stratigraphic correlation (Belyi, 1977, 1978) (Fig. 2). As such, these volcanic fields are ideal places in which to carry out a detailed geologic, geochemical, and geochronologic study of the eruptive products of the Okhotsk sector of the volcanic belt.

REGIONAL GEOLOGIC SUMMARY

The Okhotsk-Chukotka volcanic belt spans a strike length of ~3000 km extending from the Chukotka Peninsula to the mouth of the Uda River in the southwestern Sea of Okhotsk (Figs. 1, 3A). Coeval subduction-related vol-
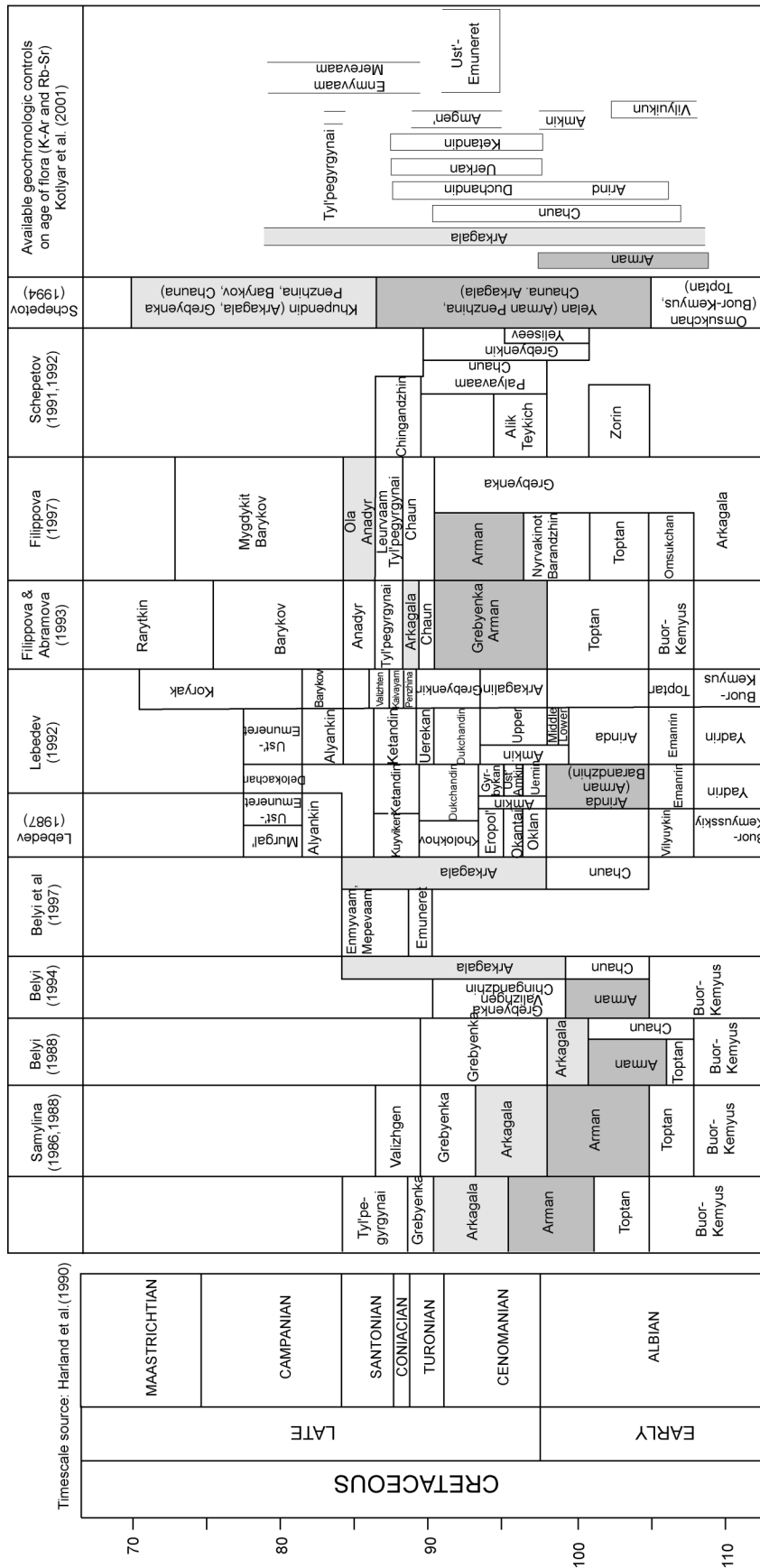
Figure 2. Compilation of stratigraphic data and chronostratigraphic correlation of floral assemblages within the Okhotsk-Chukotka volcanic belt (after Kotlyar et al., 2001). Given the disparity between previously available isotopic age designations, many workers utilize floral stratigraphy to constrain the timing of the Okhotsk-Chukotka volcanic belt. The Arman Flora (darker gray) and Arkagala flora (lighter gray) occur within the Arman and Maltan-Ola volcanic fields. There is a lack of consensus on the chronostratigraphic age of these units.
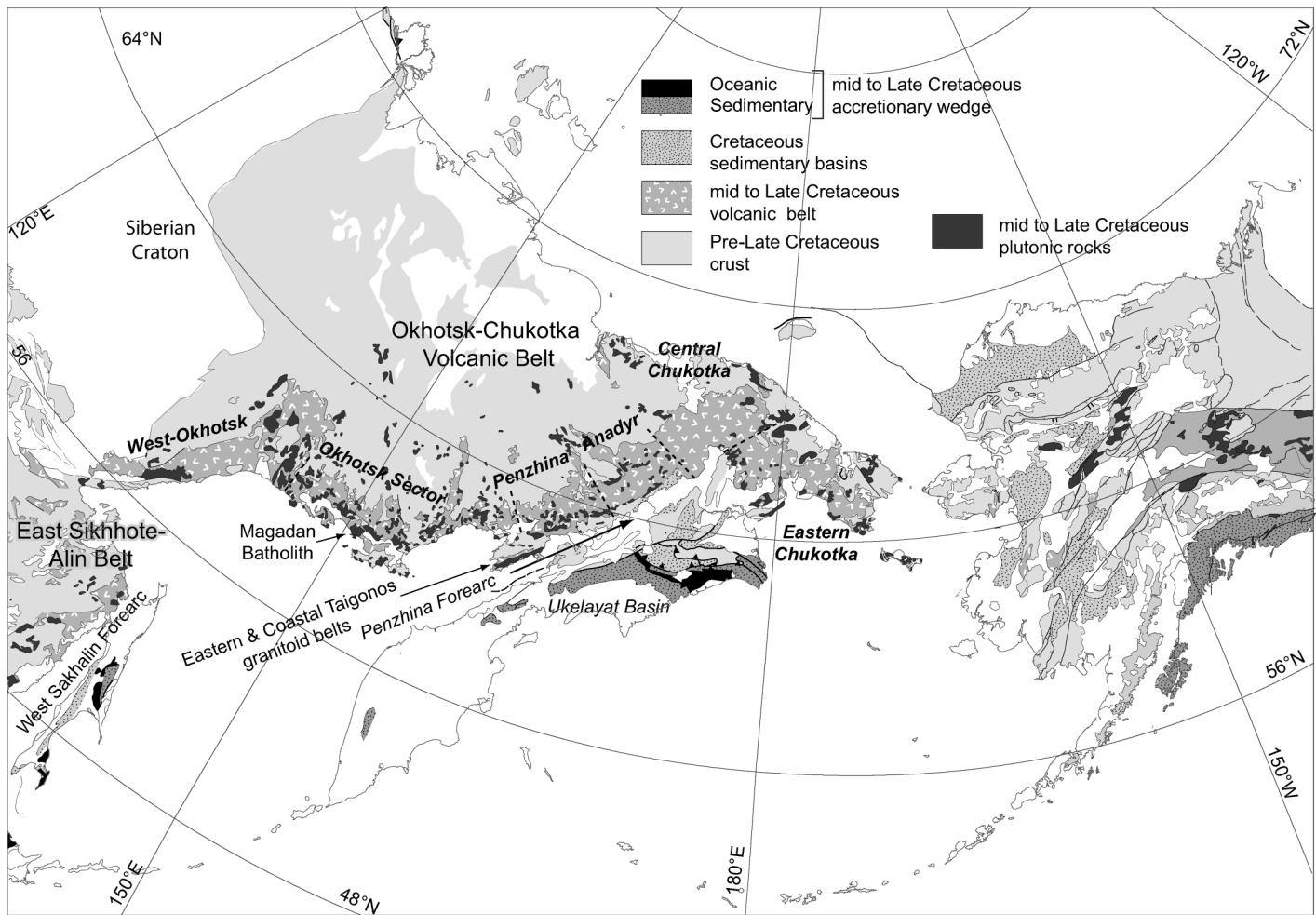
Figure 3. Circum–North Pacific tectonostratigraphic terrane map (modified from Nokleberg et al. [1998] by using a circum–North Pacific GIS [geographic information system] database compiled with data in Klemperer et al. [2002]). (A) Distribution of Andean-style magmatic arcs (Okhotsk-Chukotka volcanic belt and its sectors and Sikhote-Alin belt) and associated forearc and accretionary-prism units. (*Caption continued on p. 641.*)

canic and plutonic rocks are recognized in the Sikhote-Alin belt in Primorye (Parfenov, 1984; Zonenshain et al., 1990) as well as in eastern China (Şengör and Natal'in, 1996), suggesting the existence of an extremely widespread Andean-style magmatic arc of late Early to Late Cretaceous age. The duration of magmatic activity in the Okhotsk-Chukotka volcanic belt is debated but generally thought to encompass middle Albian to Campanian (Belyi, 1977, 1994; Parfenov, 1984; Zonenshain et al., 1990; Kotlyar et al., 2001) or Maastrichtian (Filatova, 1988) time.

The belt is subdivided into "sectors" on the basis of differences in the basement rock types and lithologic similarity of volcanic sections within specific geographic regions (Figs. 1, 3A, 3B, Belyi, 1977). From northeast to southwest, these are the Eastern Chukotka flank zone, the Central Chukotka sector, the

Anadyr sector, the Penzhina sector, the Okhotsk sector, and the Western Okhotsk flank zone (Belyi, 1977, 1978). Within the Okhotsk, Penzhina, and Central Chukotka sectors, the belt is further divided into an interior zone dominated by plutonic rocks and an exterior zone where volcanic rocks and their hypabyssal equivalents predominate (Fig. 1) (Belyy, 1977, 1978). This paper deals primarily with the volcanic rocks of the exterior zone of the Okhotsk sector of the Okhotsk-Chukotka volcanic belt (Fig. 3A).

The Okhotsk-Chukotka volcanic belt is built on heterogeneous continental and accreted island-arc crust (Fig. 3B). In the interior zone, the plutonic units intrude into metasedimentary and metavolcanic host rocks of the Jurassic–Early Cretaceous Uda-Murgal island arc (Hourigan, 2003) (Fig. 3B). In the Okhotsk sector, on the Taigonos Peninsula

(Fig. 3A), granitoids crosscut accreted ultramafic and basalt-chert sequences that record the position of the subduction zone related to Okhotsk-Chukotka volcanic belt's predecessor, the Uda-Murgal arc. In contrast, the exterior (landward) zone of the Okhotsk sector is built on deformed Permian–Jurassic marine passive-margin and backarc-basin sedimentary rocks whose metamorphic grade does not exceed low greenschist (Fig. 3B). Locally, volcanic rocks of the Okhotsk-Chukotka volcanic belt overlie flat-lying, unmetamorphosed Lower Cretaceous fluvial conglomerate and sandstone that contain volumetrically significant low-grade coal deposits. Many of the floral assemblages used to constrain the stratigraphic age of inception of Okhotsk-Chukotka magmatism occur within these coal-bearing horizons.

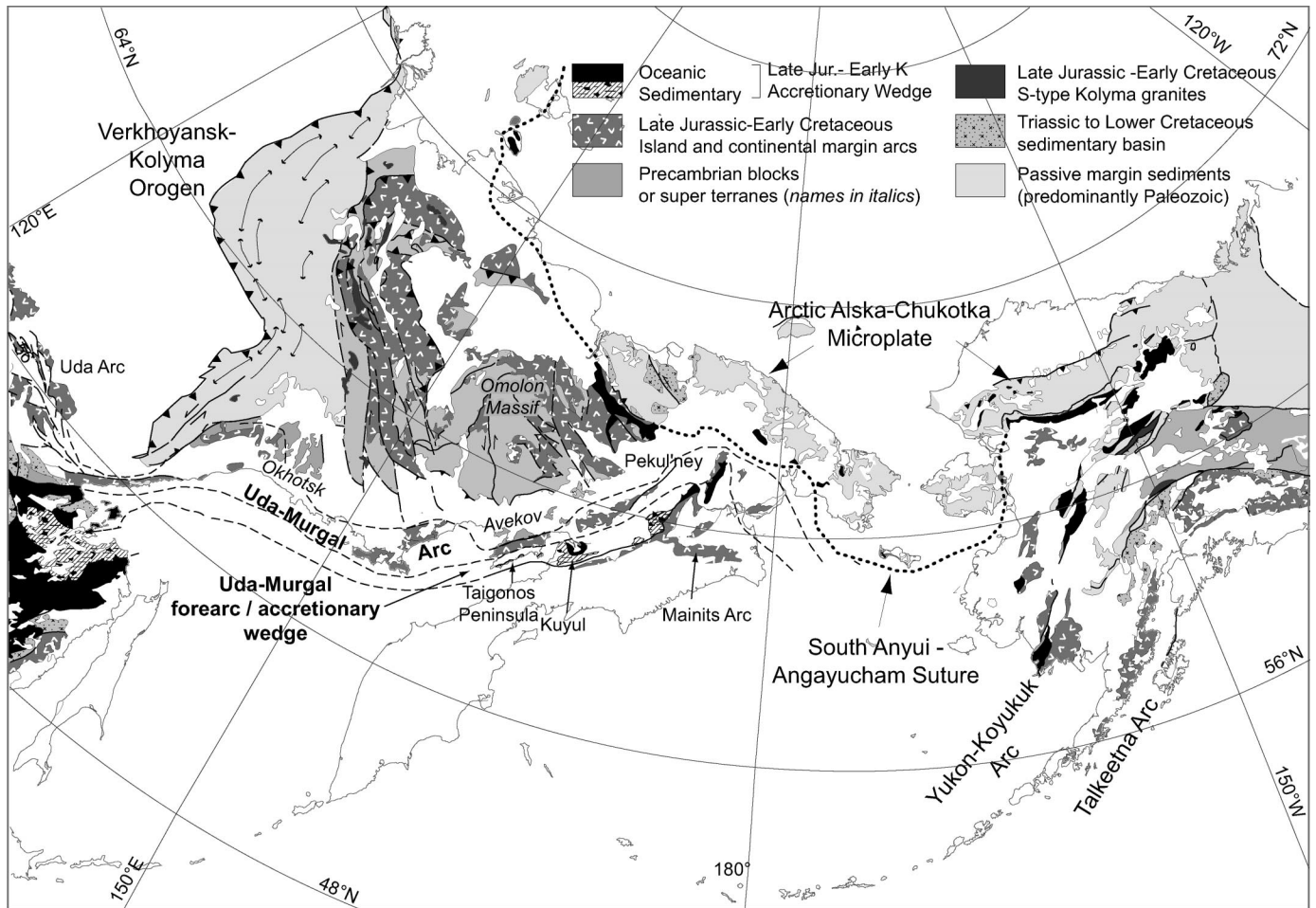The Arman volcanic field is dissected by

Figure 3. *(Caption continued from p. 640.)* **(B) Present distribution of Jurassic–Early Cretaceous island arcs and attendant convergent-margin system that predated the development of the Okhotsk-Chukotka volcanic belt.**

the Nelkandzha and Khakhandzha Rivers (Fig. 4), tributaries of the Khasyn River, ~100 km due north of Magadan (Fig. 1). The river valleys afford decent exposure of complete sections of the eruptive products of the Arman volcanic field (Fig. 4). The Maltan-Ola volcanic field is located at the divide between the Maltan and Ola Rivers, ~200 km north-northeast of Magadan (Figs. 1, 3A). Here the Kheta River exposes the contact between Late Cretaceous rhyolites and basalts and underlying folded Jurassic metasedimentary rocks.

Previous Work

Phytostratigraphy

Extant stratigraphic correlations within the Okhotsk-Chukotka volcanic belt are based on the continuous evolution of floral assemblages from mesophytic taxa (gymnosperms or ferns) in the Early Cretaceous to cenophytic taxa (angiosperms or flowering plants) in the Late

Cretaceous (e.g., Schepetov [1994] and other references cited in Fig. 2). Publications describing this work are predominantly in Russian and are not generally in international circulation. Kotlyar et al. (2001) have summarized the phytostratigraphic research to date. A modified version of the phytostratigraphic chart of Kotlyar et al. is presented in English as Figure 2 to aid the reader with the difficult nomenclature. This chart refers to work by Samylina (1974), Belyy (1982), Samylina (1986), Lebedev (1987), Samylina (1988), Schepetov (1991, 1992), Filippova and Abramova (1993), Belyi (1994), Schepetov (1994), Belyi et al. (1997), and Filippova (1997). It is beyond the scope of this work to detail these research papers except to present the reader with floral nomenclature and stratigraphic positions of individual floral assemblages.

There is little agreement about chronostratigraphy as recorded in nonmarine sedimentary sequences within the Okhotsk-Chukotka

volcanic belt (Fig. 2) The Arman and Arkagala floral assemblages, which occur within the Arman and Maltan-Ola volcanic fields (Belyi, 1977), are highlighted in light gray and dark gray in Figure 2. The Arman and Arkagala flora are generally thought to be late Albian and Cenomanian, respectively, although the ranges of each floral assemblage differ substantially between studies. Several workers (Lebedev, 1987; Filippova and Abramova, 1993) have presented chronostratigraphic scales that suggest age resolution of individual assemblages on the order of 1–2 m.y. In contrast, Schepetov (1994), noting the coexistence of the two floral assemblages (assumed to be of different age) in the same lithostratigraphic horizon, argued that the chronostratigraphic resolution afforded by the northeast Russian flora is limited to ~10 m.y. (Fig. 2).

Geochronology

The majority of existing isotopic ages from the Okhotsk-Chukotka volcanic belt are K-Ar
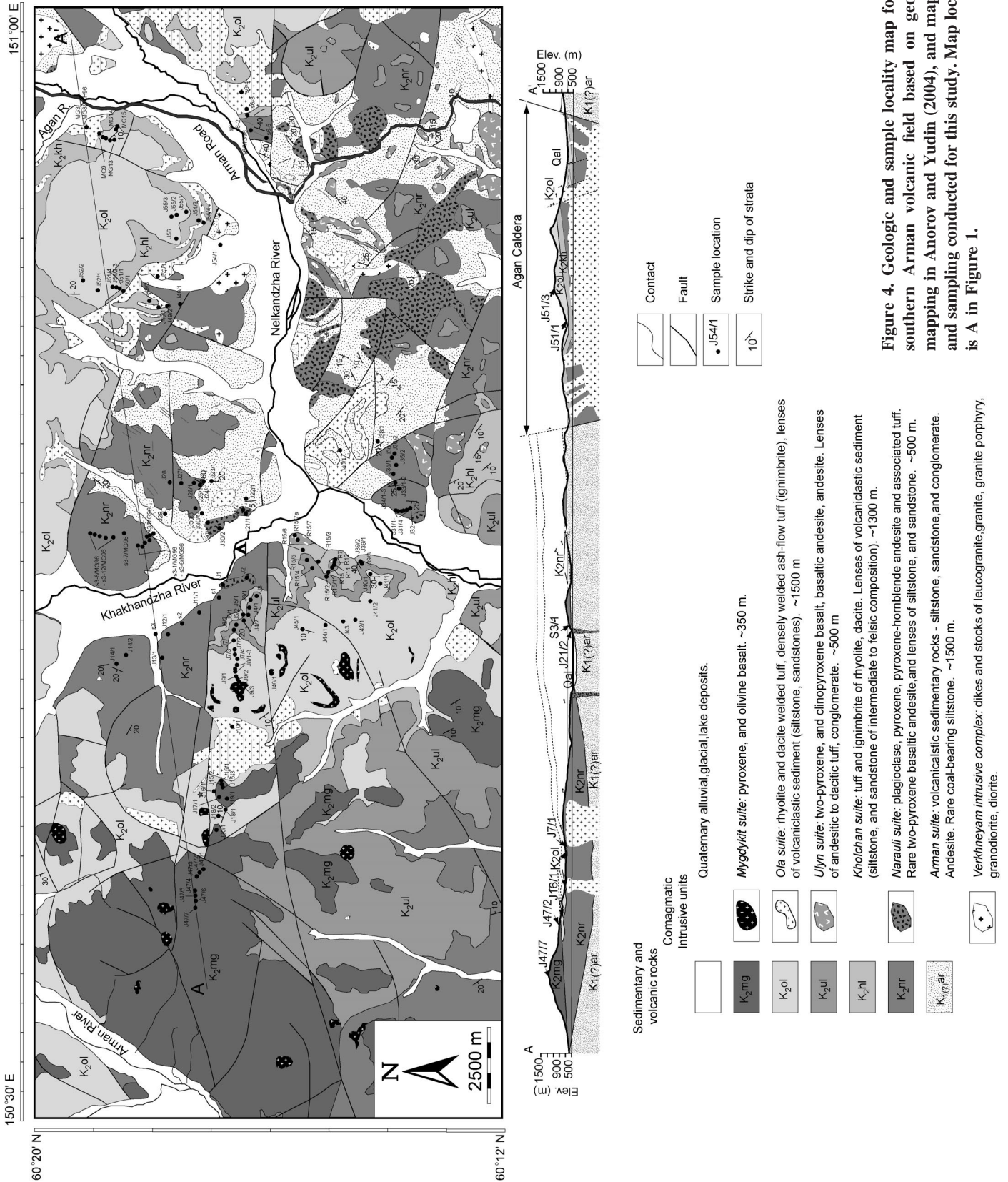
Figure 4. Geologic and sample locality map for the southern Arman volcanic field based on geologic mapping in Anorov and Yudin (2004), and mapping and sampling conducted for this study. Map location is A in Figure 1.

or Rb-Sr whole-rock isochron dates (see Kotlyar et al., 2001). These data are problematic for a number of reasons including initial isotopic disequilibrium (Rb-Sr), postemplacement open-system behavior due to alteration (Rb-Sr or K-Ar), and the potential for undetected excess argon (K-Ar). A summary of the results of Rb-Sr and K-Ar geochronology is given in Figure 2. As with phytostratigraphic ages, the available geochronology lacks acceptable temporal resolution, which likely reflects systematic problems with the isotopic methods employed rather than real, natural age ranges of these eruptive units (Fig. 2). A compilation synthesizing the available stratigraphic and geochronologic age constraints for multiple sections across the entire Okhotsk-Chukotka volcanic belt is presented as Figure DR1. The available geochronologic data generally support previous stratigraphic work (Fig. DR1); however, the geochronologic data selected to constrain the ages of these units are generally the oldest out of larger data sets following the assumption that the younger K-Ar ages might reflect open-system behavior (I.N. Kotlyar, 2002, personal commun.). This approach does not allow for the possibility of erroneous older ages due to initial isotopic disequilibrium (Rb-Sr) or excess argon (K-Ar) and thus may lead to age constraints that are too old.

Several studies have employed $^{40}Ar/^{39}Ar$ geochronometry on monomineralic separates. Kelley et al. (1999) conducted a study to bracket the age of the Chaun flora in the Central Chukotka sector of the Okhotsk-Chukotka volcanic belt (Fig. 1). Like the Arman and Arkagala flora, there is little agreement for the age of the Chaun flora (Fig. 2). Middle to late Albian (Samylina, 1988) and Turonian (Filippova and Abramova, 1993) designations represent end-member chronostratigraphic designations. Kelley et al. (1999) presented laser step-heating plateau ages for hornblende and plagioclase fractions from flows that bracket the Chaun flora in the Central Chukotka sector. Their ages are from 88.9 ± 0.8 Ma to 86.7 ± 1.4 Ma (Fig. DR1 [see footnote 1]), indicating that emplacement of these units occurred in Turonian to Santonian time rather than during Albian to Cenomanian time as argued by Samylina (1974) (Figs. 2, 3). These units are conformably overlain by sedimentary rocks containing flora of the Arkagala assemblage, which were not dated directly.

Ispolatov et al. (2000) reported several $^{40}Ar/^{39}Ar$ sanidine ages from different stratigraphic levels in two volcanic sections (Etchikun' or Kalenyvaam River drainages) in the Central Chukotka sector of the Okhotsk-Chukotka

volcanic belt (Fig. DR1 [see footnote 1]). These units also contain members of the Chaun floral assemblage. Sanidine from rhyolite and dacite within the section gives reproducible total-fusion ages for 15–20 single-crystal analyses per sample ranging from 88.0 ± 0.2 Ma to 87.1 ± 0.2 Ma (Fig. DR1). This work also corroborates the results of Kelley et al. (1999) by demonstrating an ~15 m.y. disparity between the high-precision $^{40}Ar/^{39}Ar$ geochronologic ages and the stratigraphic ages (Fig. DR1).

The disparity between $^{40}Ar/^{39}Ar$ and phytostratigraphic ages, as well as the poor resolution and reliability of K-Ar and Rb-Sr ages demonstrate the need for a revision of the chronostratigraphy of the Okhotsk-Chukotka volcanic belt. Resolution of the spatiotemporal distribution of arc magmatism is critical to understanding the nature of interaction between the paleo-Pacific oceanic plates and the northeast Asian continental margin. The volcanic belt also affords an outstanding opportunity to study a well-preserved ancient continental-margin arc. Whereas the evolutionary histories of most ancient arcs (such as the Sierra Nevada of California) are inferred from their plutonic record and/or sedimentary record within forearc basins, the upper levels of the Okhotsk-Chukotka volcanic belt are preserved practically in their entirety (despite their age) such that magmatic processes at higher levels of the crust can be studied directly.

Arman Volcanic Field

The Arman volcanic field was constructed upon low-grade metavolcanic rocks and volcaniclastic sedimentary rocks of the Lower Cretaceous Momoltykich Suite and overlying continental deposits of the Khasyn Suite (Fig. 5). Floral assemblages within the Khasyn Suite are considered Late Jurassic–Neocomian (Belyi, 1977). Stratigraphic sections from the Arman volcanic field are presented in Figure 5.

Arman Suite

Lithology. Fluviatile conglomerate of the upper part of the Arman Suite is exposed at the confluence of the Nelkandzha and Khakhandzha Rivers (Figs. 4, 5). Rounded to subrounded clasts are chiefly sandstone, shale, siltstone, and vein quartz, suggesting metasedimentary rocks of the Verkhoyansk-Kolyma orogen as the source (Fig. 3B). Up stratigraphic section, the matrix of the conglomerate becomes more tuffaceous and volcanic cobbles become more abundant (Fig. 5).

The Arman Suite exposed on the eastern bank of the Arman River south of Madaun is

the type locality for the Arman floral assemblage (Fig. 2; Fig. DR1 [see footnote 1]). On the basis of correlation with Floral Zone III of the Colville Basin (Smiley, 1969), Belyi (1977) classified the flora of the Arman floral assemblage as late Albian to Cenomanian. Lebedev (1987) related these flora exclusively to the late Albian. However, work by Schepetov (1994) has shown that some taxa in this locality did not become widespread until Turonian time, which contradicts the Albian designations assigned by previous workers. The aggregate thickness of the Arman Suite is 1700–2000 m (Fig. 5). In the upper part of the section, volcaniclastic sedimentary rocks are facies equivalents of pyroclastic flows of the Narauli Suite (Belyi, 1977). The section dips moderately along the Arman River (20°–25°NNE). Along the Nelkandzha River, the bedding dips 30°NE (Fig. 4).

Narauli Suite

Lithology. The Narauli Suite consists of pyroclastic and lava flows of andesitic composition (Figs. 4, 5, 6). Locally, these flows interfinger with fluvial conglomerates of the Arman Suite. Abundant intrusions of hornblende-plagioclase andesite crosscut the Arman and Narauli Suites, but do not cut the higher volcanic units (Fig. 4). The thickness of Narauli andesites is >1000 m (Belyi, 1977). Alteration is pervasive throughout much of the section. Massive flows in the upper parts of the section remain fresh.

Petrography. Fresh Narauli andesite flows contain phenocrysts of plagioclase (3%–10%), hornblende (2%–3%), and magnetite (1%–2%) in addition to 85% to 96% glassy groundmass. Debris flows at the base of the section tend to be more altered, containing chloritized amphibole and plagioclase phenocrysts replaced partially by sericite. For subsequent geochronologic investigation, we sampled only massive flows and plutons exposed in the upper part of the section that lacked petrographic evidence of postemplacement alteration. Even if the alteration reflects low-grade metamorphism, the temperatures were far less than the ~500 °C argon closure temperature for hornblende (e.g., McDougall and Harrison, 1999).

Geochemistry. The Narauli Suite contains a range of compositions from andesite to basaltic andesite to trachyandesite (Fig. 6A; Table DR2 [see footnote 1]). The suite spans a range of compositional fields on K_2O vs. SiO_2 variation diagrams, but moderate-K calc-alkaline varieties dominate (Fig. 6B). The location of the Narauli samples on TiO_2 vs. Zr tectonic
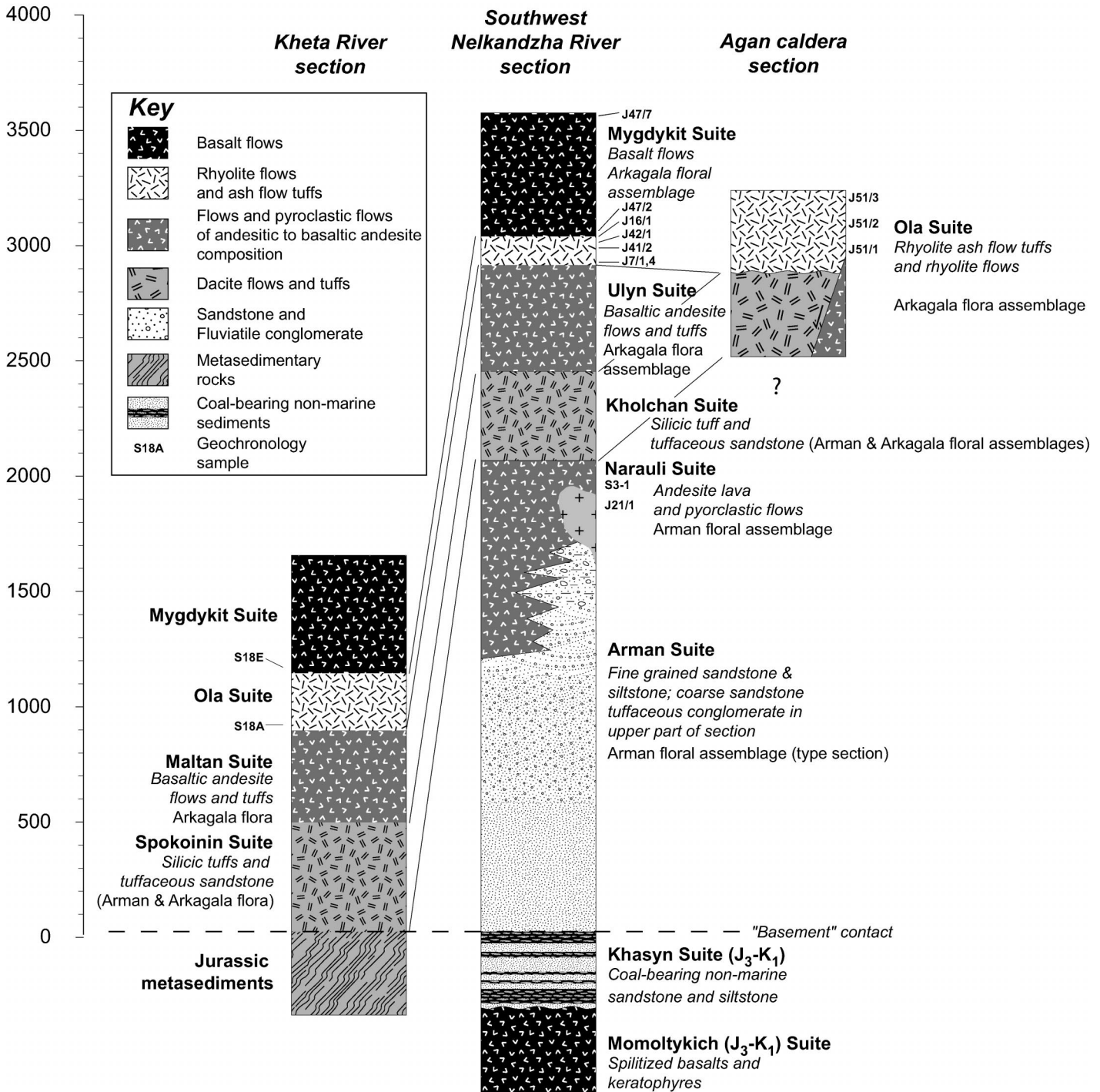
Figure 5. Lithostratigraphic columns. (A) Kheta River section in the Maltan-Ola volcanic field. (B and C) Western bank of the Nelkandzha River and Agan caldera sections, respectively, within the Arman volcanic field.
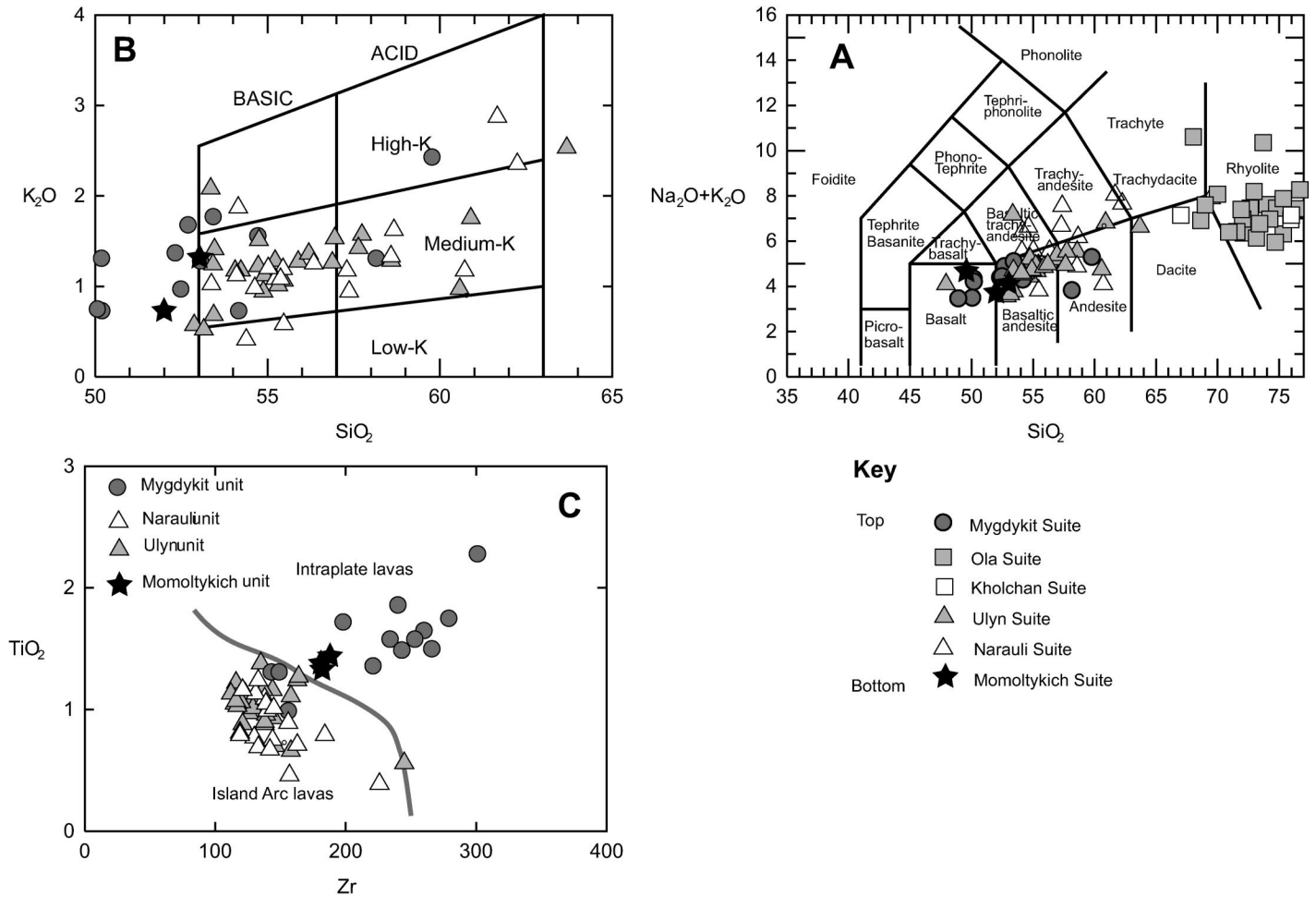
Figure 6. Geochemical diagrams for volcanic rocks within the Arman and Maltan-Ola volcanic fields. All suite symbols are given in the lower right. (A) Total alkalis vs. silica (TAS) volcanic rock classification diagram. (B) K_2O-SiO_2 variation diagram chemistry of andesites and basaltic andesites of the Arman volcanic field. Narauli and Ulyn Suites plot primarily in the field that corresponds to moderate-K calc-alkaline volcanic rocks. Mygdykit basaltic rocks plot at generally lower SiO_2 values beyond the calc-alkaline compositional range as given by Gill (1981). (C) TiO_2-Zr tectonic discrimination diagram for andesite, basaltic andesite, and basaltic lithologies in the Arman volcanic field (Pearce and Norry, 1976). Samples from the Narauli and Ulyn Suites plot in the field corresponding to subduction-related arc volcanic rocks. Mygdykit basalts plot in the within-plate basalt field. Spilitized, Early Cretaceous Momoltykich Suite basalts, which form the basement for the Arman volcanic field, also plot in the within-plate basalt field.

discrimination diagrams suggests a magmatic arc origin (Fig. 6C).

Geochronology. Two $^{40}Ar/^{39}Ar$ samples were collected from the Narauli Suite andesites. Sample S3-1 was taken from a massive flow unit in the upper part of the section (Figs. 4, 5). Sample J21/1 is from a hypabyssal hornblende-plagioclase andesite porphyry (Figs. 4, 5). Both samples yield plateau ages indicating simple closed-system behavior. Sample S3-1 yields an 85.6 ± 1.1 Ma plateau age (Fig. 7A; Table 1; Table DR3 [see footnote 1]) concordant with the inverse-isochron age of 86.2 ± 6.2 Ma associated with an atmospheric trapped $^{40}Ar/^{36}Ar$ ratio. Sample J21/2 was collected from a small pluton that crosscuts pyroclastic units of the lower Narau-

li Suite and the deposits of the Arman Suite, but does not cut the overlying Kholchan or Ulyn Suites. Hornblende from this sample yielded a plateau age of 85.5 ± 1.3 Ma (Fig. 7B; Table 1; Table DR3 [see footnote]) concordant with its isochron age (84.4 ± 2.5 Ma) for the same temperature steps. All age uncertainties are given at 2σ.

Kholchan Suite

The greatest thickness of the Kholchan Suite (Figs. 4, 5) occurs in the northern part of the Arman volcanic field (Fig. 4). The suite consists of 200–600 m of rhyolite and dacite tuffs and flows with local lenses of tuffaceous sandstone, conglomerate, and siltstone and rare andesitic tuff horizons (Belyi, 1977). Flo-

ra found within the Kholchan Suite corresponds to the Arkagala floral assemblage (I.N. Kotlyar, 2002, personal commun.). We collected one sample from the Kholchan Suite for geochemical analysis alone (Fig. 6A).

Ulyn Suite

The Ulyn Suite is composed of massive tabular flows from 1 to 10 m thick; the suite has a maximum stratigraphic thickness of 400–500 m. Flows are chiefly basaltic andesite, lesser andesite, and rare occurrences of trachyandesite (Figs. 5, 6A). These units conform to the medium-K calc-alkaline series (Fig. 6B). Ulyn Suite rocks plot in the field corresponding to arc volcanic rocks (Fig. 6C)
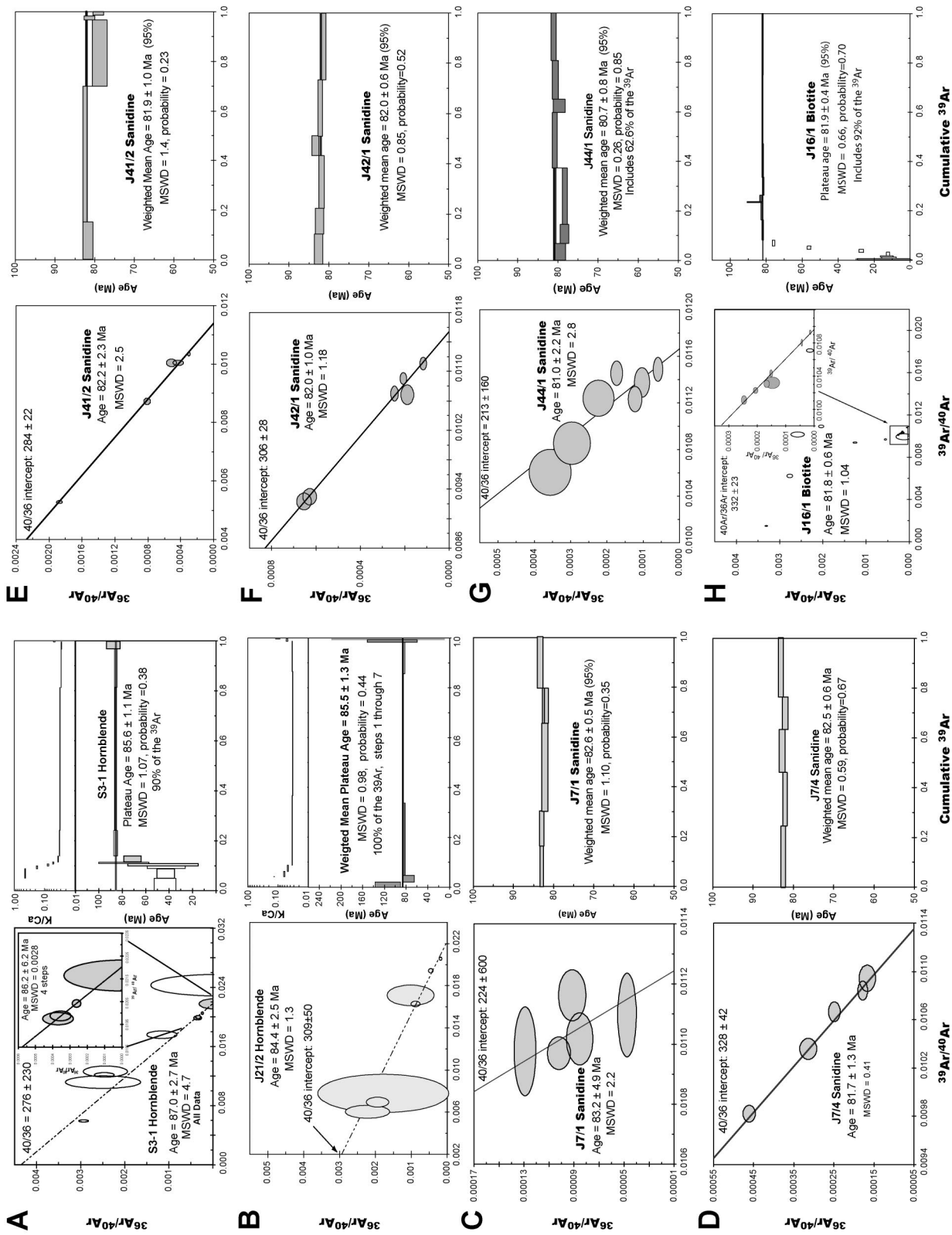
Figure 7. Inverse isochron, spectrum, and K/Ca plots for 17 new ⁴⁰Ar/³⁹Ar analyses from the Arman and Maltan-Ola volcanic fields. Spectra that were corrected for excess argon (see Appendix) are for qualitative assessment alone, as the error from uncertainty on the trapped ⁴⁰Ar/³⁶Ar ratio was not propagated. Sample localities are shown in Figure 4, and their stratigraphic position is noted in Figure 5. Data are summarized in Table 1 and detailed in Table DR3. MSWD—mean square of weighted deviates.
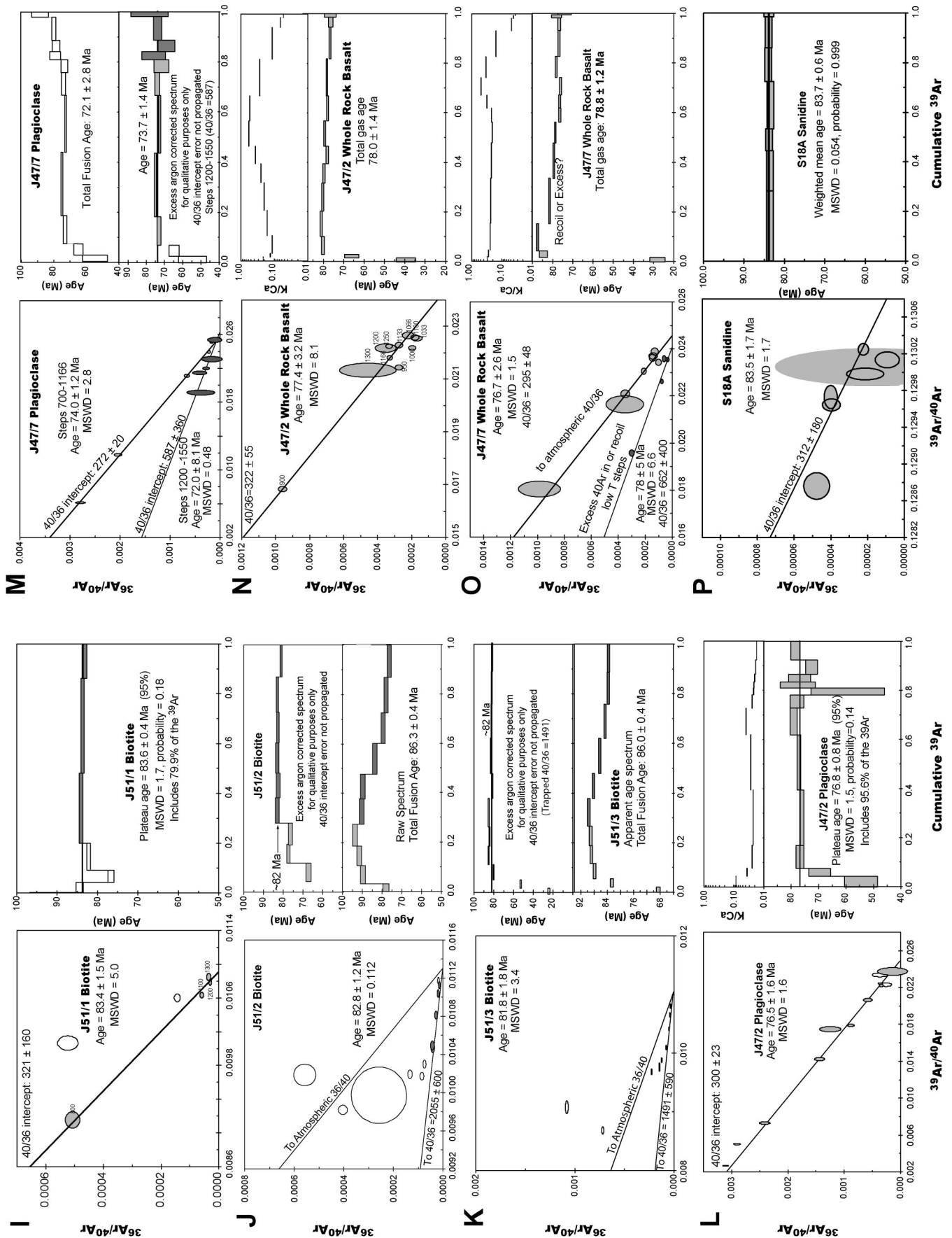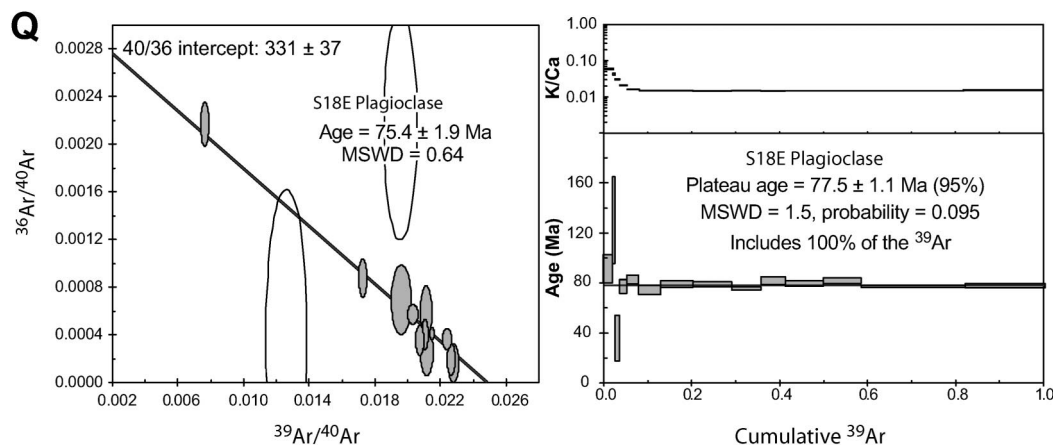
Figure 7. (*Continued.*)

Figure 7. (*Continued.*)

TABLE 1. SUMMARY OF $^{40}Ar/^{39}Ar$ GEOCHRONOLOGIC DATA

Sample number	Latitude (N)	Longitude (E)	Isochron fit				Spectrum fit			
			Isochron age (Ma)	$^{40}Ar/^{36}Ar$ intercept	MSWD	Total-fusion age (Ma)	Weighted mean age (Ma)	Plateau age (Ma)	MSWD	^{39}Ar (%)
Arman volcanic field										
Narauli Suite										
S3-1 hornblende	60°18′05″	150°45′50″	86.2 ± 6.2	276 ± 230	0.0028	80.7 ± 2.5		**85.6 ± 1.1**	1.07	90
J21/1 hornblende	60°16′30″	150°42′50″	84.4 ± 2.5	309 ± 50	1.3	85.9 ± 2.8		**85.5 ± 1.3**	0.98	100
Ola Suite										
Ash-flow tuff										
J7/1 sanidine	60°16′40″	150°38′15″	83.2 ± 4.9	224 ± 600	2.2	82.6 ± 1.4	**82.6 ± 0.5**		1.1	100
J7/4 sanidine	60°16′35″	150°37′40″	81.7 ± 1.3	328 ± 48	0.41	82.5 ± 1.2	**82.5 ± 0.6**		0.59	100
J41/2 sanidine	60°14′20″	150°39′35″	82.2 ± 2.3	284 ± 22	2.5	81.2 ± 1.0	**81.9 ± 1.0**		1.4	98
J42/1 sanidine	60°14′30″	150°39′00″	82.0 ± 1.0	306 ± 28	1.18	82.0 ± 0.7	**82.0 ± 0.6**		0.85	100
J44/1 sanidine	60°15′05″	150°38′50″	81.0 ± 2.2	213 ± 160	2.8	79.8 ± 1.6	**80.7 ± 0.8**		0.26	62.6
J16/1 biotite	60°16′50″	150°32′25″	81.8 ± 0.6	332 ± 23	1.04	*78.7 ± 0.5*		**81.9 ± 0.4**	0.66	92
Agan subunit										
J51/1 biotite	60°18′35″	150°50′10″	83.4 ± 1.5	321 ± 160	5	83.3 ± 0.8		**83.6 ± 0.4**	1.7	79.9
J51/2 biotite	60°18′38″	150°50′12″	**82.8 ± 1.2**	2005 ± 600	0.112	86.3 ± 0.8	*82.5 ± 1.4* *			
J51/3 biotite	60°18′40″	150°50′15″	**81.8 ± 1.8**	1491 ± 590	3.4	86.0 ± 0.8	*81.8 ± 0.4* *			
Mygdykit Suite										
J47/2 plagioclase	60°17′10″	150°30′28″	76.5 ± 1.6	300 ± 23	1.6	75.2 ± 2.1		**76.8 ± 0.8**	1.5	95.6
J47/2 WRB	60°17′10″	150°30′28″	77.4 ± 3.2	322 ± 55	8.1	**78.1 ± 1.4**				
J47/7 plagioclase	60°17′15″	150°29′10″								
Isochron 1			**74.0 ± 1.2**	272 ± 20	2.8	74.1 ± 2.8				
Isochron 2			72.0 ± 8.1	587 ± 360	*0.48*					
J47/7 WRB	60°17′15″	150°29′10″								
Isochron 1			76.7 ± 2.6	295 ± 48	1.5	**78.8 ± 1.2**				
Isochron 2			78.0 ± 5.0	662 ± 400	*6.6*					
Maltan-Ola volcanic field										
Ola Suite										
S18A sanidine	61°09′40″	151°36′20″	83.5 ± 1.7	312 ± 180	1.7	83.7 ± 0.8	**83.7 ± 0.6**		0.054	100
Mygdykit Suite										
S18E plagioclase	61°09′39″	151°35′50″	75.4 ± 1.9	331 ± 37	0.64	77.9 ± 2.4		**77.5 ± 1.1**	1.5	100

*See text for description of data collection, ratio calculation, and data interpretation; see Table DR2 for full data. Ages in *italics* indicate that a correction for excess argon has been performed, error from $^{36}Ar/^{40}Ar$ intercept was not propagated, and thus the isochron age is preferred. **Bold Ages** are preferred ages, underlined values denote statistically significant nonatmospheric trapped argon composition. WRB—whole-rock basalt.

on the TiO_2 vs. Zr plot (Pearce and Norry, 1976).

Ola Suite

Lithology. The Ola Suite in the Arman volcanic field comprises two units exposed on opposite banks of the Khakhandzha River (Figs. 4, 5). The section on the western bank

consists of fine-grained, crystal-poor, non-welded to moderately welded ash-flow tuffs that have a maximum thickness of 600–650 m (Fig. 5). Local tabular flows of crystal-rich rhyolite are observed in the upper part of the section. Dips do not exceed 10°. Sanidine ages reported below are from this section.

On the eastern bank of the Khakhandzha River, the high topography of the region is

supported by cliff-forming, crystal-rich welded ignimbrites (Fig. 8A) deemed the Agan caldera section (Belyi, 1977). Phenocrysts of plagioclase, quartz, biotite, and hornblende compose ~50% of the total volume. The base is densely welded and contains large (10–20 cm) fiamme (Fig. 7C). This unit is thought to represent a >350-m-thick caldera-fill sequence (Speranskaya, 1963; Yarmoluk, 1973;
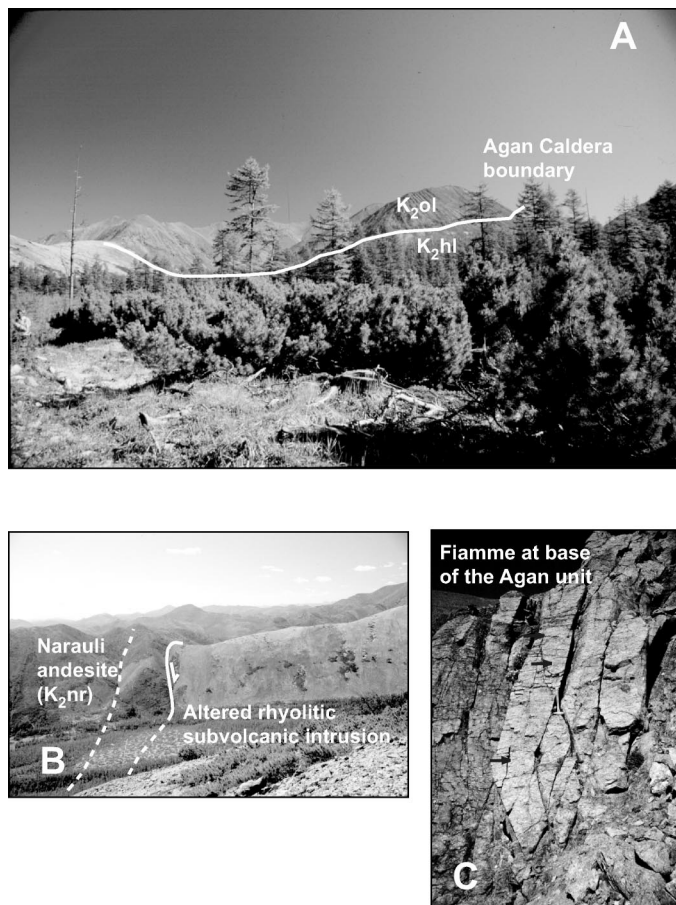
Figure 8. (A) Panorama of the volcanic section exposed on the ridge southwest of the Agan River (Fig. 4), showing the border of the Agan caldera-fill unit of the Ola Suite. (B) View looking west at north-dipping caldera-bounding faults and ring-fracture intrusions. (C) Fiamme (arrows) in welded crystal-rich rhyolite at the base of the Agan section of the Ola Suite. The field of view is approximately 3 m.

Eryomin, 1974) (Fig. 8A). The margin of the caldera is defined by steeply dipping faults that separate Narauli andesites from highly altered rhyolitic intrusive rocks. The map-scale outcrop pattern (Fig. 4) and the proximity of these intrusive rocks to the arcuate, caldera-bounding faults suggest that these rhyolitic intrusions represent ring-fracture intrusions (Fig. 8B). The Ola Suite inclusive of the Agan section is 1200–1300 m thick (Belyi, 1977) (Fig. 5). Ola Suite rhyolites are classified as moderate-K calc-alkaline rhyolites (Figs. 6A, 6B) with rare trachyte and dacite (Gill, 1981).

Geochronology. We analyzed five sanidine separates from various stratigraphic levels in the Ola Suite in the Arman volcanic field. Replicate total-laser-fusion analyses of multigrain aliquots produced high radiogenic argon yields and indicate sample homogeneity. The samples produced inverse isochrons with atmospheric ^{36}Ar/^{40}Ar intercepts and highly reproducible apparent ages (Table 1; Table DR3

[see footnote 1]). Sample J7–1 from the lowest nonwelded rhyolite tuff (Figs. 4, 5) gives an 82.6 ± 0.5 Ma sanidine age (Fig. 7C). Stratigraphically up section, J7/4 yields an 82.5 ± 0.6 Ma age (Fig. 7D). Sample J41/2 yielded a weighted mean age of these samples of 81.9 ± 1.0 Ma (Fig. 7E). J42/1 yielded reproducible ages with a weighted mean of 82.0 ± 0.6 Ma (Fig. 7F). A lone sample, J44/1, did not yield reproducible apparent ages over all steps, resulting in a young weighted mean age of 80.7 ± 0.8 Ma (Fig. 7G).

Four biotite samples from the Ola Suite were analyzed. Two samples, J51/1 and J16/1, produced plateau ages. The remaining two have hump-shaped spectra and inverse-isochron data that indicate significant excess argon (Figs. 7H–7K; Table 1; Table DR3 [see footnote 1]). Sample J16/1 was taken from an ~3-m-thick crystal-rich rhyolite flow located directly beneath the overlying Mygdykit ba-

salt. The 125–250 μm biotite fraction produced a plateau age of 81.9 ± 0.4 Ma over 92% of the gas released, concordant with an isochron age of 81.8 ± 0.6 Ma. (Fig. 7K). Sample J51/1 biotite produced a concordant spectrum and isochron ages associated with an atmospheric trapped ^{40}Ar/^{36}Ar ratio. Thus, the plateau age of 83.6 ± 0.4 Ma represents the emplacement age (Fig. 7H). Biotite from samples J51/2 and J51/3, located stratigraphically above J51/1 in the Agan caldera, exhibit excess argon in their moderate-temperature steps with initial ^{40}Ar/^{36}Ar values of 2055 and 1491. When corrected for the excess ^{40}Ar gas composition, the hump-shaped character of the spectrum is reduced. The resultant weighted mean ages are 82.5 ± 1.4 Ma and 81.8 ± 0.4 Ma (^{40}Ar/^{36}Ar fit error not propagated) (Figs. 7I, 7J; Table 1). The uncorrected total-fusion ages contradict the stratigraphic succession. Thus, we prefer inverse-isochron ages of 82.8 ± 1.2 Ma and 81.8 ± 1.8 Ma for the emplacement age of samples J51/2 and J51/3, respectively.

These new data indicate that the Ola Suite of the Arman volcanic field is of early Campanian age.

Mygdykit Suite

The Mygdykit Suite unconformably overlies the Ola Suite. Locally, the contact appears structurally discordant with evidence of erosion or weathering prior to emplacement (Fig. 4). Samples were collected over a 300 m vertical stratigraphic succession along the divide between the Arman and Nelkandzha Rivers (Figs. 4, 5). Here, the section comprises multiple flows characterized by alternating massive bases and amygdaloidal tops.

Geochronology. Samples J47/2 and J47/7 represent the basal (0 m) and upper (300 m) flows of the Mygdykit Suite, respectively. The samples were collected from the massive basal section of their respective flow units because they contain petrographically pristine phenocrystic plagioclase. Companion groundmass concentrate analyses were performed for each of these samples. J47/2 plagioclase yields a plateau age of 76.8 ± 0.8 Ma over 96% of the ^{39}Ar released (Fig. 7L, Table 1). Sample J47/7 plagioclase is somewhat more complex. A two-isochron model best fits the data. The low- and moderate-temperature steps define a linear array with an atmospheric ^{40}Ar/^{36}Ar composition. The high-temperature steps produce a well-defined linear array with excess argon (the ^{40}Ar/^{36}Ar ratio is 587 ± 360) (Fig. 7M). Modeling complex isochron data as two domains associated with differing trapped argon gas compositions is common practice and
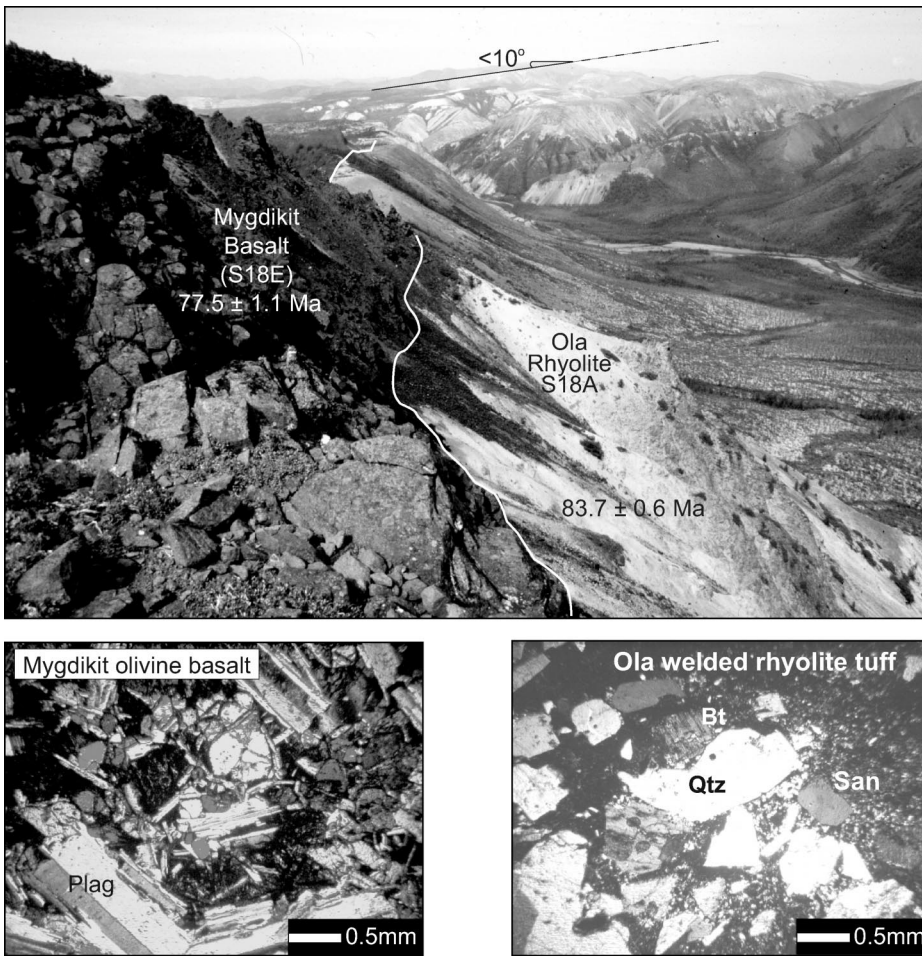
Figure 9. Panorama of the Kheta River valley. Densely welded to nonwelded rhyolitic ash-flow tuffs of the Ola Suite make up the white to slightly pinkish-buff slopes in the foreground and far slope. Erosional remnants of olivine basalts of the Mygdykit Suite occur sporadically above the Ola rhyolite. Rhyolitic section dips <10° to the south. Photomicrographs show mineral phases used for ^{40}Ar/^{39}Ar geochronology (plag—plagioclase, bt—biotite, san—sanidine, qtz—quartz).

is described in more detail by Heizler and Harrison (1988). We prefer the isochron age of 74.0 ± 1.2 Ma because no assumption of initial ^{40}Ar/^{36}Ar composition is required for age calculation.

The groundmass-concentrate data are more difficult to interpret. The whole-rock sample of the lower basalt flow (J47/2) did not yield a true plateau. The total gas (78.0 ± 1.4 Ma) and isochron ages (Fig. 7N; 77.4 ± 3.2 Ma) are concordant with the plagioclase age, helping to corroborate the 76.8 ± 0.8 Ma age of this flow as given by the plagioclase data. Sample J47/7 whole-rock data exhibit a hump-shaped spectrum. We applied a two-isochron model to the data. The moderate-temperature steps reflect excess argon (the ^{40}Ar/^{36}Ar ratio is 662 ± 400) (Fig. 7O). Because these are groundmass concentrates, the hump-shaped

spectra may alternatively reflect ^{39}Ar recoil from glass and microphenocrysts. An isochron age of 76.7 ± 2.6 Ma is favored for sample J47/7 because it is concordant with the plagioclase inverse-isochron age and chronostratigraphically consistent with other systematically less complex ages lower in the section.

The data indicate that emplacement of the lower Mygdykit Suite basalts began at 76.8 ± 0.8 Ma. The plagioclase data from the uppermost mapped flow unit suggest that basaltic magmatism was active through 74.0 ± 1.2 Ma. A comparison of our ^{40}Ar/^{39}Ar data with whole-rock K-Ar analyses of these same specimens carried out at SVKNII (North East Interdisciplinary Scientific Research Institute) in Magadan, Russia, is instructive. Sample J47/2 and J47/7 yielded ages 71.8 ± 1.8 Ma and 87.5 ± 2.5 Ma, respectively (I.N. Kotlyar,

2002, personal commun.). We suggest that the age disparity is best explained by argon loss due to devitrification in sample J47/2 and by excess argon in sample J47/7 perhaps preserved in argon-rich fluid inclusions in olivine and pyroxene phenocrysts (McDougall and Harrison, 1999).

Maltan-Ola Volcanic Field (Kheta River Section)

Ola Suite

The Ola and Mygdykit Suites are exposed along the Kheta River valley (Figs. 1, 5) where they unconformably overlie Jurassic metasedimentary rocks (Fig. 5). Locally, rhyolites of the Ola Suite conformably overlie fluvial conglomerates made up chiefly of subrounded andesite clasts. In this section, the Ola Suite comprises 200–300 m of welded to nonwelded white to reddish, vapor-phase–altered rhyolite ash-flow tuffs (Figs. 5, 9). Sanidine from this section was petrographically pristine.

Geochronology. Sanidine from one welded rhyolite tuff (S18A) was separated and analyzed. These data are isochronous, yield atmospheric trapped argon gas compositions, and a weighted mean age of replicate multigrain total-fusion analyses of 83.7 ± 0.6 Ma (Fig. 7P).

Mygdykit Suite
Lithology. The contact between the Mygdykit Suite basalt and the Ola Suite rhyolite is conformable and sharp. Basalt flows occur as cliff-forming units or scattered erosional remnants (Fig. 9). The thickness of the Mygdykit Suite section in the Maltan-Ola field ranges from 450 to 800 m (Belyi, 1977). Sedimentary rocks of the Pervomai Suite, which contain Arkagala flora, occur at the contact between the Ola and Mygdykit Suites elsewhere in the Maltan-Ola field (e.g., I.N. Kotlyar, 2002, personal commun.) (Fig. 2 and Fig. DR1 [see footnote 1]).

Geochronology. A plagioclase separate from sample S18E yielded a plateau age of 77.5 ± 1.1 Ma with an mean square of weighted deviates (MSWD) of 1.5 (Fig. 7Q). The data are isochronous over the temperature steps that define the plateau associated with an atmospheric trapped argon gas composition. This result is in agreement with the eruption ages of the Mygdykit unit in the Arman volcanic field.
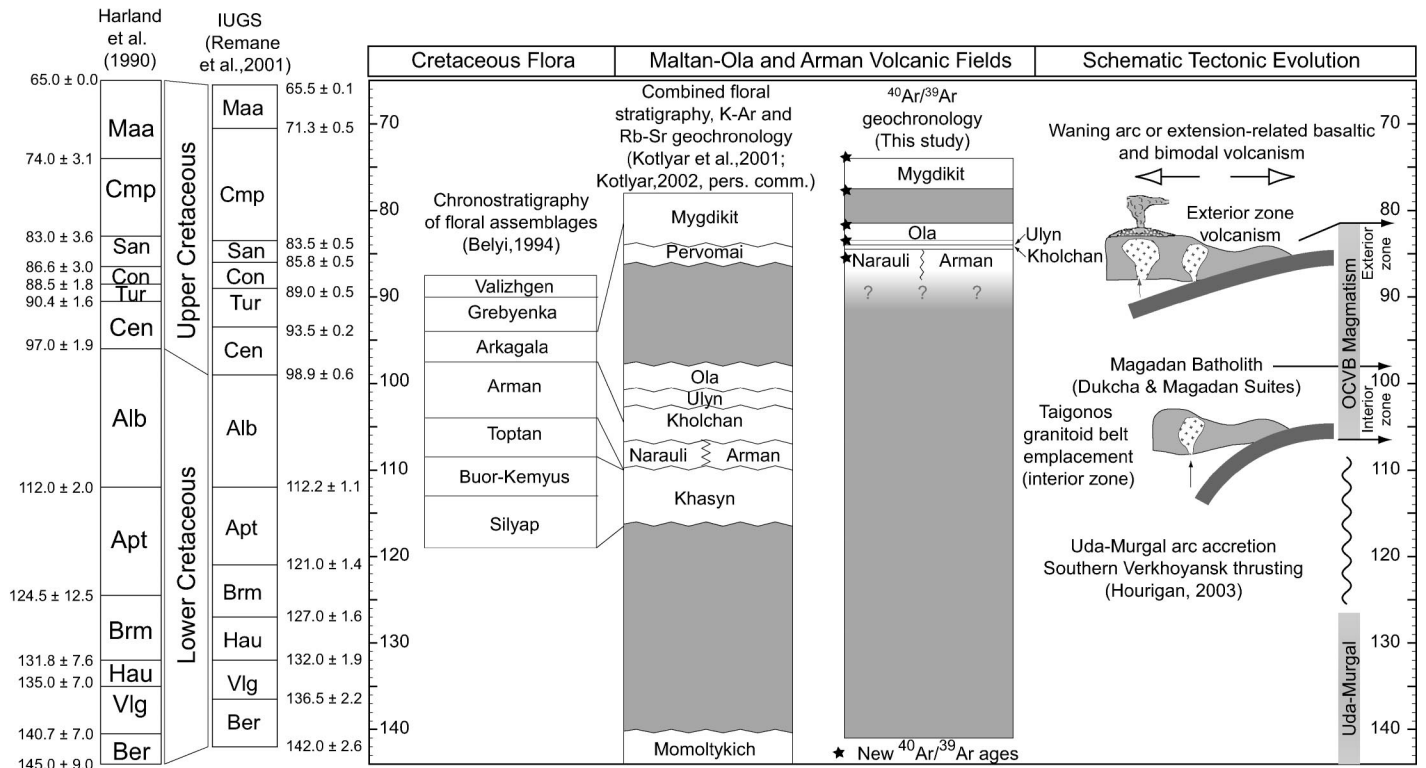
Figure 10. Summary of chronostratigraphic data. Column 1 gives chronostratigraphic scheme for the various floral assemblages recognized in the Cretaceous nonmarine sedimentary rocks of northeastern Russian (after Belyi, 1994). Column 2 is the chronostratigraphy of the Arman region produced by synthesizing the previously published floral stratigraphy and geochronology (after I.N. Kotlyar, 2002, personal commun.; Fig. 2; Fig. DR1 [see footnote 1 in the text]). Tie lines connect floral assemblages to volcanic units in which they are found. Column 3 summarizes the results of the geochronologic component of this investigation. There is an ~15 m.y. disparity between the previous chronostratigraphic schemes and those indicated by the $^{40}Ar/^{39}Ar$ geochronologic data in this study. Column 4 is a schematic tectonic evolution model to explain the observed spatiotemporal distribution of subduction-related volcanic and plutonic rocks in the Okhotsk sector of the Okhotsk-Chukotka volcanic belt. Shallowing of the downgoing plate may explain the observed continentward migration of the axis of arc magmatism during the Late Cretaceous.

DISCUSSION

Chronostratigraphic Implications

The $^{40}Ar/^{39}Ar$ data presented here suggest that the emplacement of most of the subduction-related volcanic section in the Arman volcanic structure occurred from 85.6 ± 1.3 Ma to 80.7 ± 0.8 Ma (Fig. 10). Capping basaltic volcanism occurred from 77.5 ± 1.1 Ma to 74.0 ± 1.2 Ma after an ~3 m.y. hiatus.

The Narauli andesite flow unit places a minimum age on the emplacement of the Narauli Suite as a whole at 85.5 ± 1.3 Ma (2σ). Because the floral-bearing Arman Suite interfingers with the upper part of the Narauli Suite, the Santonian chronostratigraphic age designation indicates inaccuracy in the Albian age that was assigned on the basis of previous phytostratigraphic and geochronologic investigations (Fig. 2 and references therein; Fig. 10). Our data do not preclude that Arman flora

may be as old as Albian, but they necessitate that the flora is younger than previously recognized. Other instances of chronostratigraphic disparity have been reported by Kelley et al. (1999) and Ispolatov et al. (2000), who argued that the floral age designations are 15 m.y. too old.

The Ola Suite is known to contain flora of the Arkagala assemblage and yields $^{40}Ar/^{39}Ar$ ages ranging from 83.7 ± 0.6 Ma to 80.7 ± 0.8 Ma. Previous research suggested that the Arkagala flora within the Ola Suite is early Cenomanian age (see references in Fig. 2). Here too, the Campanian stratigraphic age indicated by the $^{40}Ar/^{39}Ar$ geochronology documents systematic inaccuracy in the age designation of the Arkagala floral assemblage. Arkagala flora is also found in the Mygdykit basalt units, which range in age from 77.5 ± 1.1 Ma to 73.7 ± 0.7 Ma, suggesting that these taxa survived through at least the late Campanian (Fig. 10). These data suggest that

the chronostratigraphic age range of the Arkagala flora in the Okhotsk sector should be revised to Santonian–Campanian (Fig. 10).

With growing concerns about global climate change, significant attention has been focused on understanding the climatic record through time by studying preserved flora in continental deposits. Northeastern Russia and Alaska host a great abundance of well-preserved Cretaceous nonmarine sections. Where fresh, datable volcanic rocks and fossiliferous sedimentary rocks are interbedded, there is outstanding opportunity to resolve the chronostratigraphy to <1 m.y. for Cretaceous samples (~1% relative standard error). Detailed high-precision $^{40}Ar/^{39}Ar$ geochronology will greatly improve our understanding of the age of these deposits and ultimately improve Cretaceous paleoclimatic models (e.g., Herman and Spicer, 1996; Kelley et al., 1999). This study represents an important step for our growing understanding of the climatic record

in northeastern Russia by documenting systematic discrepancies between phytostratigraphic and $^{40}Ar/^{39}Ar$ ages. Collaborative, multidisciplinary research on the Okhotsk-Chukotka volcanic belt shows great promise for helping to resolve Cretaceous climatic changes in the northwest Pacific region as well as improving our understanding of the tectonic and magmatic evolution of the northeast Asian continental margin.

Tectonic Implications

Spatiotemporal Patterns of Arc Magmatism

Constraining the spatiotemporal patterns of magmatism is important for the overall understanding of the evolution of the margin and nature of subduction along the northeast Asian margin. This work, combined with other recent studies on the timing of magmatism on the Taigonos Peninsula, permits a summary of a model for the evolution of the Okhotsk sector of the Okhotsk-Chukotka volcanic belt presented in Figure 10. On the Taigonos Peninsula, emplacement of the Eastern Taigonos and Coastal Taigonos granitoid belt occurred between 106.5 ± 1.6 Ma and 97.0 ± 1.1 Ma according to zircon U-Pb ages from undeformed granitoids (Hourigan, 2003) (Fig. 10). The Dukchin and Magadan Suites, the youngest recognized intrusive units of the Magadan batholith (Andreeva and Izokh, 1990), yield 97.4 ± 1.0 Ma and 96.8 ± 1.2 Ma zircon U-Pb ages, respectively (Fig. 10). These data indicate that magmatic activity in the interior zone of the Okhotsk-Chukotka volcanic belt began during Albian time, following accretion of the Uda-Murgal island arc, and continued through to Cenomanian time (Hourigan, 2003). Although the available U-Pb and $^{40}Ar/^{39}Ar$ ages are insufficient in quantity and distribution to resolve the time-space patterns of magmatism in great detail, the available data point to an ~200 km continentward migration of the axis of arc magmatism over 20 m.y. The data also suggest a magmatic hiatus between late stages (Andreeva et al., 1997) of the intrusion of the Magadan batholith at 97 Ma (Hourigan, 2003) and emplacement of the volcanic rocks described in this paper at 86 Ma. Continentward migration of the axis of arc magmatism in the Late Cretaceous (Fig. 10) may be explained by shallowing of the downgoing paleo-Pacific slab. Fast spreading at the Kula Ridge at 85 Ma (e.g., Engebretson et al., 1985), coincident with the onset of exterior-zone magmatism, may have led to faster, shallower subduction beneath northeast Asia.

The Mygdykit Basalt: What Caused Arc Cessation?

The Mygdykit Suite basalts of the Maltan-Ola and Arman volcanic fields were erupted over a 3–4 m.y. period beginning at 77.5 ± 1.1 Ma and continuing to 74.0 ± 1.2 Ma after an ~3 m.y. magmatic hiatus, according to the $^{40}Ar/^{39}Ar$ geochronology of plagioclase separates reported here. On TiO_2 vs. Zr tectonic discrimination diagrams, the basalts correspond to within-plate basalts (Pearce and Norry, 1976), suggesting that the Mygdykit Suite is temporally and geochemically distinct from the Okhotsk-Chukotka volcanic belt. Filatova (1985, 1988) argued that these basaltic units were exposed margin-wide in a linear array of depressions subparallel to the margin. On the basis of this regional geologic relationship and some additional geochemical work, Filatova (1985, 1988) concluded that the Mygdykit and its equivalents represent a rift-related volcanic sequence. This sequence was assigned a Paleogene age on a regional geologic map (Gorodinskyi, 1980); however, in several localities beyond the Okhotsk sector, the capping basalt units contain the Arkagala floral assemblage and thus likely constitute Campanian equivalents of the Mygdykit section.

Polin and Moll-Stalcup (1999) presented a detailed geochemical investigation of the capping basalts in the Central Chukotka sector and Eastern Chukotka flank zone of the Okhotsk-Chukotka volcanic belt (Fig. 1; Fig DR1 [see footnote 1]), which are considered stratigraphic equivalents of the Mygdykit basalts (Gorodinskyi, 1980). These capping units share many of the geochemical features of intraplate basalts (trachybasalts) and rift-margin magmatism (alkaline granite, comendite), suggesting an extension-related tectonic setting (Polin and Moll-Stalcup, 1999). During our mapping in the Arman volcanic field, we did not observe normal faults that were active synchronously with Mygdykit basalt eruption, although the discontinuity at the Ola-Mygdykit contact may represent an episode of minor faulting. The fact that the volcanic rocks are flat lying and the section is preserved nearly in its entirety suggests that the Okhotsk-Chukotka volcanic belt was never a high-standing arc sequence like the modern Andes, nor was there major shortening deformation with attendant tilting of the volcanic section. This observation indicates a tectonic setting that is at least ''neutral'' and possibly ''extensional'' for the waning phase of arc magmatism.

The extension-related petrogenetic and regional tectonic model for the Mygdykit basalt contradicts the prevailing model for the ces-

sation of Okhotsk-Chukotka magmatism. It has been generally accepted that a microcontinental block (Parfenov and Natal'in, 1977; Zonenshain et al., 1990; Şengör and Natal'in, 1996) or oceanic plateau (Watson and Fujita, 1985; Bogdanov and Dobretsov, 2001) collided with the margin, preventing further subduction, which led to a cessation of subduction-related magmatic activity in Late Cretaceous time. In theory, the collision of a sizeable, rigid tectonic block should produce significant shortening-related deformation, including tilting of the volcanic section and deposition of synorogenic sedimentary rocks (e.g., Ontong-Java Plateau or Yakutat block) (Cloos, 1993). However, there is no evidence of the inferred Late Cretaceous collision on land, where all the late-stage volcanic rocks are flat lying (see Figs. 4 and 9) and no synorogenic sedimentary rocks are preserved. Offshore, the available seismic reflection data show an early Tertiary extensional history with no evidence for pre-Tertiary contractional deformation (Hourigan, 2003). Given the facts that (1) the geology on land does not record a collisional event, and (2) the geochemistry of the Mygdykit basalts indicates a waning arc or extensional tectonic setting for magmatism, we argue that arc cessation cannot have been caused by the collision of a microcontinent with the northeast Asian margin. In this light, models for the evolution of the northeast circum-Pacific, and in particular, for the origin of the Sea of Okhotsk, will have to be reevaluated.

CONCLUSIONS

$^{40}Ar/^{39}Ar$ ages from systematically sampled volcanic units of the Arman and Maltan-Ola volcanic fields document the inaccuracy of previous age designations for the Arman and Arkagala floral assemblages. Narauli Suite ages of 85.6 ± 1.3 Ma and 85.5 ± 1.1 Ma indicate that the Arman floral assemblage persisted into Santonian time, 13 m.y longer than previously thought (references in Fig. 2). The age of the Arkagala floral assemblage must be revised to Santonian–Campanian on the basis of ages from the Ola and Mygdykit Suites that range from 83.7 ± 0.8 Ma to 74.0 ± 1.4 Ma.

The geochronologic data suggest that the volcanic activity in the Arman volcanic field was relatively short-lived. Although the lowest flows of the Narauli Suite were not dated because of alteration, the base of the section is probably <1.0 m.y. older than the 85.5 Ma age obtained for the upper flow because individual volcanic edifices typically span tens to hundreds of thousands of years. Medium-

K, calc-alkaline magmatism in this field continued until ca. 81 Ma, suggesting that the volcanic succession of the Arman Volcanic field was emplaced over ~5 m.y.

The Mygdykit basalts are geochemically and temporally distinct from the underlying section of volcanic rocks in the Okhotsk-Chukotka volcanic belt. The geochronologic data indicate an ~3 m.y. hiatus in magmatic activity followed by ~4 m.y. of basaltic volcanism from 77.5 ± 1.1 Ma to 74.0 ± 1.2 Ma. The shift in geochemistry of the lavas from calc-alkaline volcanic arc to within-plate, possibly extension-related magmas (Polin and Moll-Stalcup, 1999) also supports this distinction. We suggest that the capping basalt unit be omitted from a formal definition of the Okhotsk-Chukotka volcanic belt.

The within-plate character of the basaltic volcanism and the lack of deformation of the Okhotsk-Chukotka volcanic belt and its margin are inconsistent with the prevailing tectonic models, which suggest that arc cessation was the result of the collision of a nonsubducting microcontinent or oceanic plateau. New tectonic models are required to explain the cessation of the Okhotsk-Chukotka volcanic belt in the absence of such a collisional event.

APPENDIX: METHODOLOGY

Samples for $^{40}Ar/^{39}Ar$ analysis were selected in the field on the basis of the lack of alteration at the outcrop and hand-sample scales. Prior to separation, thin sections of each sample were studied to confirm the lack of alteration at the microscopic level. Hornblende, plagioclase, biotite, and sanidine concentrates were obtained by using standard mineral-separation techniques, including crushing, grinding, Frantz magnetic separation, and heavy liquids. Basaltic groundmass concentrates were obtained from the 250–100 μm fraction that behaved magnetically at 0.5 A with a 15° forward slope and a 10° side-slope and nonmagnetically at 0.1 A with the same slope parameters. This method removes olivine phenocrysts that commonly contain excess argon in fluid inclusions and lack radiogenic argon because of absence of potassium (McDougall and Harrison, 1999). All samples were handpicked under a binocular microscope to achieve purity and rinsed with acetone and deionized water to remove surface contaminants. For each sample, 2–20 mg was packaged in high-purity copper foil and stacked vertically in a quartz vial with intermittently spaced packets of Taylor Creek rhyolite sanidine fluence monitors (85G003: 27.88 Ma (Duffield and Dalrymple, 1990); TCR2: 27.87 Ma, M. Lanphere, 2000, written commun.). Vials were irradiated at the Oregon State University Triga reactor in the cadmium-shielded CLICIT facility. Ages reported here are from samples irradiated in three separate irradiations ranging in duration from 2 to 16 h.

J-values were calculated from laser-fusion analyses of several multiple-grain aliquots of Taylor Creek rhyolite sanidine. Weighted mean *J*-values for monitor packets spaced every fifth packet within the vial were used to interpolate *J*-values for unknowns. Isotopic measurements were performed at the Stanford University Noble Gas Geochronology Lab. Gas extraction was accomplished by using a fully automated Staudacher-type, double-vacuum resistance furnace (biotite, hornblende, plagioclase, and groundmass concentrates) or by a multigrain-aliquot laser fusion using a 10 W argon-ion laser (sanidine). Evolved gas was purified by using two SAES-ST172 getters at ~4.0 A (275 °C) for periods of 5–12 min prior to inlet into the spectrometer. Peaks were measured by using a Mass Analyzer Products 216 noble-gas mass spectrometer with a Johnson MM1 electron multiplier with a Baur-Signer source. The sensitivity of the spectrometer for typical gain values is ~4.75 × 10⁻¹³ mol·V⁻¹. Each measurement consisted of 7–20 cycles through the run table consisting of *m/e* (mass divided by charge) of 40, 39, 38, 37, 36, 35.5 (baseline). The entire measurement protocol is automated by using a custom-designed LABVIEW 5.1 code written by Mike McWilliams and Jeremy Hourigan. Typical machine blanks at *m/e* = 40 are 7.5 × 10⁻¹⁶ mol at <1000 °C and 1.5 × 10⁻¹⁵ mol at 1400 °C.

Raw data were trimmed and regressed to inlet time by using Eyesorecon written by Bradley Hacker. Ratios were corrected for machine blanks, decay, and interference by using an in-house Excel workbook routine. For irradiation S40, ³⁷Ar decay and ³⁶Ar$_{Ca}$ interference corrections were not performed because of the long delay between irradiation and measurement. We report only data from phases with high K/Ca ratios (i.e., biotite and sanidine) for irradiation S40, such that the effect of omitting the ³⁶Ar$_{Ca}$ interference correction is negligible. Isochron plots and ages, release spectra, and plateau ages were produced with Isoplot v. 2.49 (Ludwig, 1999). Both the Excel data processing routine and Isoplot v. 2.49 use a ⁴⁰K decay constant of 5.543 × 10⁻¹⁰ s⁻¹ (Steiger and Jager, 1978).

Samples that yield plateau ages meet the following basic criteria imposed by Isoplot v. 2.49: (1) The plateau consists of three or more contiguous steps that comprise >60% of the total ³⁹Ar released. (2) Probability of fit of the plateau is >0.05 (i.e., steps are concordant at the 95% confidence interval). (3) There is no resolvable slope on the plateau. (4) There are no outliers or trends in the upper and lower steps. The inverse-isochron plot provides a critical test for the assumption inherent in the age-spectrum plots that the trapped argon gas has an atmospheric isotope composition (i.e., ⁴⁰Ar/³⁶Ar = 295.5). Concordance of inverse-isochron ages defined by isochronous (i.e., low MSWD) data and plateau ages is a final criterion for defining a ''true plateau'' age (Dalrymple and Lanphere, 1974). In several cases, excess argon (i.e., trapped argon with ⁴⁰Ar/³⁶Ar > 295.5 at the 2σ confidence interval) was observed for data defining a statistically robust linear array in an inverse isochron plot. In these cases we cite the inverse-isochron age as the preferred age.

ACKNOWLEDGMENTS

REFERENCES CITED

Andreeva, N.V., and Izokh, A.P., 1990, Intrusive series of the Magadan massif and criteria of their identification: Magadan, Russia, North East Interdisciplinary Scientific Research Institute, Far East Branch, Russian Academy of Sciences, 83 p. (in Russian).

Andreeva, N.V., Davydov, I.A., and Lyuksin, A.D., 1997, Main stage of intrusive magmatism in northern Priokhot'ya and its age by the results of isotope dating, *in* Magmatism and mineralization in northeast Russia: Magadan, Russia, North East Interdisciplinary Scientific Research Institute, Far East Branch, Russian Academy of Sciences, p. 175–191.

Anorov, P.N., and Yudina, G.M., 2004, Gosudarstvennaya geologicheskaya karta Rossiiskoi Federazii (Government geological map of the Russian Federation), 2nd Edition Magadan Series P-56-XXXI (Palatka): Saint Petersburg, All-Russian Research Geological Institute (in press).

Belyi, V.F., 1977, Stratigrafiya i struktury Okhotsko-Chukotskogo vulkanogennogo poyasa [Stratigraphy and structure of the Okhotsk-Chukchi volcanic belt]: Moscow, Nauka, 275 p. (in Russian).

Belyi, V.F., 1978, Formatsii i tektonika Okhotsko-Chukotskogo vulkanogennogo poyasa [Formations and structural geology of the Okhotsk-Chukchi volcanic belt]: Moscow, Nauka, 211 p. (in Russian).

Belyi, V.F., 1988, Aktualniye voprosi fitostratigrafii ''srednego'' mela Severo-Vostoka SSSR, (Actual question on the phytostratigraphy of the ''middle'' Cretaceous, North-East, USSR: Magadan, Russia, North East Interdisciplinary Scientific Research Institute, Far East Branch, Academy of Sciences of the USSR, 34 p. (in Russian).

Belyi, V.F., 1994, Geologiya Okhotsko-Chukotskogo volcanogennogo poyasa [Geology of the Okhotsk-Chuklotka volcanic belt]: Magadan, Russia, North East Interdisciplinary Scientific Research Institute, Far East Branch, Russian Academy of Sciences, 76 p. (in Russian).

Belyi, V.F., Raikevish, M.I., and Belaya, B.V., 1997, Pozdnyaya stadiya razvitiyiya severnoi chasti Okhotsko-Chukotskogo volcanogennogo poyasa [Late stage of the development of the northern part of Okhotsk-Chukotka volcanic belt]: Stratigrafiya, Geologicheskaya Korrelyatsiya, v. T5, p. 78–89 (in Russian).

Belyy, V.F., 1982, K probleme vozrasta Okhotsko-Chukotskogo vulkanogennogo poyasa [Problem of the age of Okhotsk-Chukchi volcanic belt]: Tikhookeanskaya Geologiya = Pacific Geology, v. 1982, no. 3, p. 101–109.

Bogdanov, N.A., and Dobretsov, N.L., 2001, Okhotsk oceanic volcanic plateau, *in* 7th Zonenshain International Conference on Plate Tectonics: Moscow, Nauchnyi Mir, p. 498.

Bogdanov, N.A., and Dobretsov, N.L., 2002, The Okhotsk volcanic plateau: Russian Geology and Geophysics, v. 43, no. 2, p. 87–99 (English translation).

Cloos, M., 1993, Lithospheric buoyancy and collisional orogenesis: Subduction of oceanic plateaus, continental margins, island arcs, spreading ridges, and seamounts: Geological Society of America Bulletin, v. 105, p. 715–737.

Dalrymple, G.B., and Lanphere, M.A., 1974, ⁴⁰Ar/³⁹Ar age

spectra of some undisturbed terrestrial samples: Geochimica et Cosmochimica Acta, v. 38, p. 715–738.

Duffield, W.A., and Dalrymple, G.B., 1990, The Taylor Creek Rhyolite of New Mexico: A rapidly emplaced field of lava domes and flows: Bulletin of Volcanology, v. 52, p. 475–487.

Engebretson, D.C., Cox, A., and Gordon, R.G., 1985, Relative motions between oceanic and continental plates in the Pacific Basin: Geological Society of America Special Paper 206, 59 p.

Eryomin, R.A., 1974, Gidrotermal'nyi metamorphism i orudenenie Armanskoi vulkanostruktury [Hydrothermal metamorphism and ores of Arman volcanic structure]: Novosibirsk, Nauka, 134 p.

Filatova, N.I., 1985, Tectonic position of Maestrichtian–Eocene basaltoid magmatism in the northwestern part of the Pacific Ocean belt: Geotectonics, v. 21, p. 359–372.

Filatova, N., 1988, Perioceanic volcanic belts: Moscow, Nedra, 264 p. (in Russian).

Filippova, G.G., 1997, Stratigrafiya i vozrast kontinental'nikh otolozhenii basseina peki Amguema i severnogo poberezh'ya zaliva Kresta [Stratigraphy and age of non-marine deposits of the Amguem river basin and northern coast of the Kresta Gulf]: Kolyma, v. 2, p. 12–27. (in Russian).

Filippova, G.G., and Abramova, L.N., 1993, Pozdnemelovaya flora Severo-Vostoka Rossii [Late Creteceous flora of northeast Russia]: Moscow, Nedra, 348 p.

Gill, J.B., 1981, Orogenic andesites and plate tectonics: Berlin, Springer, 389 p.

Gnibidenko, H.S., and Khvedchuk, I.I., 1982, The tectonics of the Okhotsk Sea: Marine Geology, v. 50, p. 219–261.

Gorodinskyi, M.E., 1980, Geologicheskaya Karta Severo-Vostoka SSSR [Geologic map of the northeast of USSR]: Ministry of Geology of the USSR, scale 1: 1,500,000.

Harland, W.B., Armstrong, R.L., Cox, A.V., Craig, L.E., Smith, A.G., and Smith, D.G., 1990, A geologic time scale, 1989: Cambridge, Cambridge University Press, 263 p.

Heizler, M.T., and Harrison, T.M., 1988, Multiple trapped argon isotope components revealed by 40Ar/39Ar isochron analysis: Geochimica et Cosmochimica Acta, v. 52, p. 1295–1303.

Herman, A.B., and Spicer, R.A., 1996, Palaeobotanical evidence for a warm Cretaceous Arctic Ocean: Nature, v. 380, p. 330–333.

Hourigan, J.K., 2003, Mesozoic–Cenozoic tectonic and magmatic evolution of the northeast Russian margin [Ph.D. thesis]: Stanford, California, Stanford University, 257 p.

Ispolatov, V.O., Tikhomirov, P.L., and Cherpanova, I.Y., 2000, Noviye 40Ar/39Ar danniye o vozraste Okhtosko-Chukotskovo volcanogennogo poyasa (tsentral'no Chukotskskiy sector) [New 40Ar/39Ar data on the age of the Okhotsk-Chukotka volcanic belt (Central Chukotka sector)], in Isotopic dating of geologic processes: New methods and results: Moscow, Institute of Geology of Ore Deposits, Petrography, Mineralogy and Geochemistry, Russian Academy of Sciences (IGEM-PAN), p. 159–161 (in Russian).

Kelley, S.P., Spicer, R.A., and Herman, A.B., 1999, New 40Ar/39Ar dates for Cretaceous Chauna Group tephra, north-eastern Russia, and their implications for the geologic history and floral evolution of the North Pa-

cific region: Cretaceous Research, v. 20, no. 1, p. 97–106.

Klemperer, S.L., Greninger, M.L., and Nokleberg, W.J., 2002, Geographic information system compilation of geophysical, geologic and tectonic data for the Bering Shelf, Chukchi Sea, Arctic margin and adjacent landmasses, in Miller, E.L., Grantz, A., and Klemperer, S.L., eds., Tectonic evolution of the Bering Shelf–Chuckchi Sea–Arctic margin and adjacent landmasses: Boulder, Colorado, Geological Society of America Special Paper 360, p. 359–374.

Kotlyar, I.N., Zhulanova, I.A., Pusakova, T.B., and Gagieva, A.M., 2001, Isotopniye sistemi: Magmaticheskikh i metmorphicheskikh kompleksov severo-vostoka rossii [Isotopic systems: Magmatic and metamorphic complexes of northeast Russia]: Magadan, Russia, North East Interdisciplinary Scientific Research Institute, Far East Branch, Russian Academy of Sciences, 319 p. (in Russian).

Lebedev, Y.L., 1987, Stratigrafiya i vozrast Okhotsko-Chukotskogo vulkanogennogo poyasa [The stratigraphy and age of the Okhotsk-Chukchi volcanic belt]: Moscow, Geologicheskiy Institut, v. 421, p. 176.

Lebedev, Y.L., 1992, Melovye flory Severo-Vostoka Azii, (Cretaceous flora of Northeast Asia) Izvestiya Akademii Nauk SSSR: Seriya Geologicheskaya 4, p. 85–96 (in Russian).

Ludwig, K.R., 1999, User's manual for Isoplot/Ex version 2, A geochronological toolkit for Microsoft Excel, Special Publication 1a: Berkeley, California, Berkeley Geochronology Center, 47 p.

McDougall, I., and Harrison, T.M., 1999, Geochronology and thermochronology by the 40Ar/39Ar method: Oxford, Oxford University Press, 269 p.

Nokleberg, W.J., Parfenov, L.M., Monger, J.W.H., Norton, I.O., Khanchuk, A.I., Stone, D.B., Scholl, D.W., and Fujita, K., 1998, Phanerozoic tectonic evolution of the Circum–North Pacific: U.S. Geological Survey Open-File Report 98–0754, 125 p.

Parfenov, L.M., 1984, Kontinental'niye okrainy i ostrovniye dugi mezozoid severo-vostoka azii [Continental margins and island arcs of the Mesozoid of north-east Asia]: Novosibirsk, Nauka, 183 p.

Parfenov, L.M., and Natal'in, B.A., 1977, Mesozoic–Cenozoic tectonic evolution of northeastern Asia: Transactions (Doklady) of the USSR Academy of Sciences: Earth Science Sections, v. 235, no. 1–6, p. 89–91.

Pearce, J.A., and Norry, M.J., 1976, Petrogenesis implications of Ti, Zr, Y, and Nb variations in volcanic rocks: Contributions to Mineralogy and Petrology, v. 69, p. 33–47.

Polin, V.F., and Moll-Stalcup, E.J., 1999, Petrologo-geokhimicheskie kriterii tektonicheskikh uslovii formirovaniye Chukotskovo zvena Okhotsko-Chukotskogo volcanicheskogo poyasa [Petrologic-geochemical criteria of the tectonic conditions of formation of the Chukotka section of the Okhtosk Chukotka volcanic belt]: Tikhookeanskaya Geologiya = Pacific Geology, v. 18, no. 4, p. 29–47 (in Russian).

Remane, J., Faure-Muret, A., and Odin, G.S., 2001, International stratigraphic chart: UNESCO, IUGS, 1 sheet.

Samylina, V.A., 1974, Rannemeoloviye flory Severo-Vostoka SSSR (K probleme stanovleniya flory Kainofita) [Early Cretaceous flora of northeast USSR (Toward the problem of development of Cenophytic flora)]: Leningrad, Nauka, 56 p.

Samylina, V.A., 1986, Korrelyatsiya kontinental'nykh melovykh otlozheniy Severo-Vostoka SSSR [Correlation of the Cretaceous terrestrial sediments of the northeastern USSR]: Sovetskaya Geologiya, v. 1986, no. 6, p. 43–53.

Samylina, V.A., 1988, Arkagalinskaya stratoflora Severo-Vostoka Azii [Arkagalinian stratoflora of northeastern Asia]: Leningrad, Nauka, 131 p. (in Russian).

Schepetov, S.V., 1991, Srednemelovaya flora Chaunskoi serii (Tsentral'naya Chukotka) [Middle Cretaceous flora of the Chaun series (Central Chukotka)]: Magadan, Russia, North East Interdisciplinary Scientific Research Institute, Far East Branch, Russian Academy of Sciences, 50 p. (in Russian).

Schepetov, S.V., 1992, Srednemolovaya flora pravoberezh'ya p. Anadyr' [Mid-Cretaceous flora of the right bank of the Anadyr River]: Magadan, Russia, North East Interdisciplinary Scientific Research Institute, Far East Branch, Russian Academy of Sciences, 161 p. (in Russian).

Schepetov, S.V., 1994, Problemi paleofloristicheskogo metoda v stratigrafii (Problems of the paleoflora method in stratigraphy), in Pokhialainen, V.P., ed., Materiali po stratigrafii kontinental'nogo mela Severo-Vostoka Russii (Material on the Cretaceous non-marine stratigraphy of northeast Russia): Magadan, Russia, North East Interdisciplinary Scientific Research Institute, Far East Branch, Russian Academy of Sciences, p 49–53.

Şengör, A.M.C., and Natal'in, B.A., 1996, Paleotectonics of Asia: Fragments of a synthesis, in Yin, A., and Harrison, M., eds., The tectonic evolution of Asia: London, Cambridge University Press, p. 486–641.

Smiley, C.J., 1969, Cretaceous floras of Chandler-Colville region, Alaska—Stratigraphy and preliminary floristics: American Association of Petroleum Geologists Bulletin, v. 53, p. 482–502.

Speranskaya, I.M., 1963, O prirode svyasi ignimbritov s blispoverchnostnymi intrusiyami granitoidov [About nature of connection of ignimbrites with subvolcanic intrusions of granites]: Izvestiya vuzov, Ser. Geol. and Razvedka, v. 4, p. 3–16 (in Russian).

Steiger, R.H., and Jager, E., 1978, Subcommission on Geochronology: Convention on the use of decay constants in geochronology and cosmochronology, in Cohee, G.V., Glaessner, M.F., and Hedberg, H.D., eds., Contributions to the geologic time scale: Tulsa, American Association of Petroleum Geologists, p. 67–71.

Watson, B.F., and Fujita, K., 1985, Tectonic evolution of Kamchatka and the Sea of Okhotsk: Implications for the Pacific Basin, in Howell, D.G., ed., Tectonostratigraphic terranes of the Circum-Pacific region: Houston, Texas, Circum-Pacific Council for Energy and Mineral Resources, p. 333–348.

Yarmoluk, V.V., 1973, Vulkanicheskie struktury obrusheniya Okhotsko-Chukotskogo vulkanitcheskogo poyasa [Volcanic collapse structures of Okhotsk Chukotka volcanic belt]: Novosibirsk, Nauka, 104 p. (in Russian).

Zonenshain, L.P., Kuzmin, M.I., Natapov, L.M., and Page, B.M., 1990, Geology of the USSR: A plate-tectonic synthesis: American Geophysical Union Geodynamics Series, v. 21, 242 p.